This article has not been copyedited and formatted. The final version may differ from this version.
Molecular Pharmacology Fast Forward. Published on January 9, 2013 as doi:10.1124/mol.112.081695

SOMATIC MUTATIONS IN GRM1 IN CANCER ALTER METABOTROPIC GLUTAMATE RECEPTOR 1 INTRACELLULAR LOCALIZATION AND SIGNALING

Jessica L. Esseltine, Melinda D. Willard, Isabella H. Wulur, Mary E. Lajiness, Thomas D. Barber, and Stephen S. G. Ferguson

Molecular Brain Research Group, Robarts Research Institute and Department of Physiology and Pharmacology, University of Western Ontario, London, Ontario N6A 5K8 (JLE, SSGF)
Tailored Therapeutics, Eli Lilly and Company, Indianapolis, IN, USA (MDW, IHW,MEH) TDB)

Molecular Pharmacology Fast Forward. Published on January 9, 2013 as DOI: 10.1124/mol.112.081695
This article has not been copyedited and formatted. The final version may differ from this version.

RUNNING TITLE: SOMATIC MUTATIONS IN GRM1 ALTER RECEPTOR ACTIVITY

Correspondence should be addressed to Dr. S. S. G. Ferguson, Robarts Research Institute, University of Western Ontario, 100 Perth Dr., London, Ontario, Canada, N6A 5K8, Tel.: 519-931-5706; Fax: 519-931-5252, ferguson@robarts.ca.

Number of text pages: 35
Number of figures: 10
Number of tables: 1
Number of references: 49
Number of words in Abstract: 243
Number of words in Introduction: 719
Number of words in Discussion: 1089

Nonstandard abbreviations: HEK – Human Embryonic Kidney, GPCR – G Protein-Coupled Receptor, GRK – G protein-coupled Receptor Kinase, mGluR1a – metabotropic Glutamate Receptor 1a, IP – Inositol Phosphate, HA – Hemaglutinnin, GFP/YFP – Green/Yellow Fluorescent Protein, PAGE – Polyacrylamide Gel Electrophoresis, PBS – Phosphate Buffered Saline, HBSS – Hanks Balanced Salt Solution

Molecular Pharmacology Fast Forward. Published on January 9, 2013 as DOI: 10.1124/mol.112.081695
This article has not been copyedited and formatted. The final version may differ from this version.

ABSTRACT

The activity of metabotropic glutamate receptors (mGluRs) is known to be altered as the consequence of neurodegenerative diseases such as Alzheimer's, Parkinson's and Huntington's disease. However, little attention has been paid to this receptor family's potential link with cancer. Recent reports indicate altered mGluR signalling in various tumour types, and several somatic mutations in mGluR1a in lung cancer were recently described. Group 1 mGluRs (mGluR1a and mGluR5) are primarily coupled to Gαq leading to the activation of phospholipase C, the formation of diacylglycerol and inositol 1,4,5-trisphosphate leading to release of Ca^{2+} from intracellular stores and PKC activation. In the present study, we investigated the intracellular localization and G protein-dependent and -independent signalling of 8 *GRM1* (mGluR1a) somatic mutations. Two mutants found in close proximity to the glutamate binding domain and cysteine-rich region (R375G and G396V) show both decreased cell surface expression and basal inositol phosphate formation. However, R375G shows increased ERK1/2 activation in response to quisqualate stimulation. A mutant located directly in the glutamate binding site (A168V) shows increased quisqualate-induced IP formation, and similar to R375G, increased ERK1/2 activation. Additionally, a mutation in the GRK2/PKC regulatory region (R696W) shows decreased ERK1/2 activation, while a mutation within the Homer binding region in the carboxyl-terminal tail (P1148L) does not alter the intracellular localization of the receptor it induces changes in cellular morphology and exhibits reduced ERK1/2 activation. Taken together, these results suggest mGluR1a signalling in cancer is disrupted by somatic mutations with multiple downstream consequences.

Molecular Pharmacology Fast Forward. Published on January 9, 2013 as DOI: 10.1124/mol.112.081695
This article has not been copyedited and formatted. The final version may differ from this version.

INTRODUCTION

Metabotropic glutamate receptors mediate the actions of the excitatory neurotransmitter, glutamate. These class C receptors are characterized by a large extracellular amino-terminal glutamate binding region comprised of two globular domains which form a distinctive “venus fly trap” (VTF) (Conn and Pin, 1997). The specific amino-terminal glutamate binding region has been identified as a stretch of 24 amino acids whose mutations affect glutamate affinity (Dhami and Ferguson, 2006; O’Hara et al., 1993). Adjacent to the VFT domain is a 70 amino acid cysteine-rich domain required for allosteric coupling between the VFT and the transmembrane domains (Huang et al., 2011). This region also participates in receptor dimerization via the formation of a cysteine bridge between receptor pairs, the disruption of which leads to receptor loss of function (Romano et al., 1996).

The second intracellular loop of mGluR is involved in G protein coupling and selectivity (Pin et al., 1994). Group 1 mGluRs (mGluR1a and mGluR5) primarily couple through Gαq and also activate G protein-independent signal transduction pathways including mitogen-activated kinases. Group I mGluR-mediated ERK1/2 activation can occur via PKC, β-arrestin, non-receptor tyrosine kinases, such as Src and Pyk2, and Homer (Emery et al., 2010; Nicodemo et al., 2010; Thandi et al., 2002; Mao et al., 2005).

Receptor activation is quickly followed by signal desensitization, a tightly regulated process essential to prevent aberrant signalling or chronic receptor overstimulation (Ferguson, 2007). Desensitization of mGluRs is complex as mGluR1a desensitization includes phosphorylation-dependent and -independent mechanisms (Ferguson, 2007; Dhami and Ferguson, 2006; Dhami et al., 2005, Dhami et al., 2004; Ribeiro et al., 2009). GRK2-mediated mGluR1/5 desensitization is phosphorylation-independent, whereas, second messenger-dependent kinases phosphorylate the second intracellular loop and carboxyl-terminal tail

Molecular Pharmacology Fast Forward. Published on January 9, 2013 as DOI: 10.1124/mol.112.081695
This article has not been copyedited and formatted. The final version may differ from this version.

domains of mGluR1a to mediate phosphorylation-dependent mGluR desensitization (Francesconi and Duvoisin, 2000; Ciruela et al., 1999).

GPCR C-tails are responsible for association with many regulatory proteins involved in protein scaffolding and/or transport. For example, the Homer family of proteins is comprised of three family members each encoding multiple splice variants (Shiraishi-Yamaguchi and Furuichi, 2007). Homers associate with the PPxxFR motif in the C-tails of mGluR1a/5 via their amino-terminal ENA/VASP homology domains and regulate the subcellular distribution, plasma membrane target and signalling of mGluR1a/5 (Ango et al., 2002; Roche et al., 1999; Tadokoro et al., 1999). Homer proteins tether mGluR1a/5 to the activation of IP receptors, ERK1/2 phosphorylation and the modulation of ion channel activity (Mao et al., 2005; Kammermeier et al., 2000; Yamamoto et al., 2005; Ango et al., 2011).

mGluRs have recently been found to play a role in cancer progression (Teh and Chen, 2012). This finding is unsurprising as mGluRs can activate both MAPK and AKT, two of the hallmark signalling pathways that promote cancer growth, survival, invasion and angiogenesis in tumours. Along these lines, overexpression and/or activating mutations of mGluR1, mGluR5 and mGluR3 in various cancer types such as breast, melanoma, and RCC have been shown to promote tumour development, growth and progression, and pharmacologic inhibitors of these receptors correlates with reduced tumorigenesis (Polluck et al., 2003; Ohtani et al., 2008; Abdel-Daim et al., 2010; Prickett et al., 2011; Choi et al., 2011; Martino et al., 2012; Speyer et al., 2012). Thus, mGluRs appear to play a critical role in maintenance of the transformed phenotype and could be potential therapeutic targets for the treatment of several cancers.

Recently, whole exome sequencing of multiple tumour types has identified over 20 somatic missense mutations in the ligand binding and intracellular regulatory domains of mGluR1a (Table 1) (Kan et al., 2010; Parsons et al., 2008; Sjoblom et al., 2006; Wood et al., 2007). In the present study, we examined the effect of eight *GRM1* single nucleotide variants (SNVs) identified in glioblastoma, lung and colorectal cancer including: SNVs in the orthosteric

Molecular Pharmacology Fast Forward. Published on January 9, 2013 as DOI: 10.1124/mol.112.081695
This article has not been copyedited and formatted. The final version may differ from this version.

glutamate binding region (D44E and A168V) and cysteine-rich region of the amino-terminal domain (R375G and G396V), intracellular loop 2 (R684C, R696W and G688V) and Homer binding motif (P1148L) on mGluR1a signalling. Therefore, we asked the question whether these naturally occurring mutations alter the expected signal transduction properties, protein interactions and subcellular localization of mGluR1a. We find that a subset of these mutations result in altered mGluR1a-stimulated G protein-coupling, biased ERK1/2 phosphorylation, intracellular retention in the endoplasmic reticulum (ER), and a loss of Homer binding. Each of these alterations in mGluR1a signaling phenotype has the potential to contribute to altered receptor activity in cancer.

Molecular Pharmacology Fast Forward. Published on January 9, 2013 as DOI: 10.1124/mol.112.081695
This article has not been copyedited and formatted. The final version may differ from this version.

MATERIALS AND METHODS

Materials

myo-(^{3}H)Inositol was acquired from PerkinElmer Life Sciences (Waltham, MA). Dowex 1-X8 (formate form) resin 200–400 mesh was purchased from BioRad (Mississauga, ON, Canada). Normal donkey serum was purchased by Jackson ImmunoResearch (West Grove, PA, USA). ECL Western blotting detection reagents were purchased from GE Healthcare (Oakville, ON, Canada). Horseradish peroxidase-conjugated anti-rabbit and anti-goat IgG secondary antibody were obtained from BioRad (Mississauga, ON, Canada) and anti-mGluR1a rabbit polyclonal antibody purchased from Upstate (Lake Placid, NY, USA). Rabbit polyclonal phospho-p42/44 MAP kinase (Thr202/Tyr402), p42/44 MAP kinase antibodies were obtained from Cell Signaling Technology (Pickering, ON, Canada). Alexa Fluor 488 donkey anti-Rabbit IgG, Alexa Fluor 568 donkey anti-rabbit IgG and Zenon Rabbit Alexa Fluor 555 were purchased from Invitrogen/Molecular Probes (Burlington, ON, Canada). Rabbit anti-FLAG antibody, M2 anti-FLAG agarose, Rabbit anti-HA antibody, and all other biochemical reagents were purchased from Sigma-Aldrich (Oakville, ON, Canada).

DNA Construction

To create the pcDNA3.1(+)/FLAG-mGluR1a constructs, amino acids 19-1194 of human mGluR1a were cloned in-frame with the signal peptide from the transmembrane receptor CD33 (amino acids 1-15) followed by a single FLAG tag (DYKDDDDK). Site-directed mutagenesis was performed using the QuikChange system (Stratagene) to generate the following mutants of mGluR1a: D44E, A168V, R375G, G396V, R684C, G688V, R696W, and P1148L.

Cell Culture

Human embryonic kidney (HEK) 293 cells were maintained in Eagle's minimal essential medium supplemented with 8% (v/v) heat inactivated fetal bovine serum (Invitrogen, Burlington,

Molecular Pharmacology Fast Forward. Published on January 9, 2013 as DOI: 10.1124/mol.112.081695
This article has not been copyedited and formatted. The final version may differ from this version.

ON) and 50 μg/ml gentamicin. Cells seeded in 100 mm dishes were transfected using a modified calcium phosphate method as described previously (Dale et al., 2001). Following transfection (18 h), the cells were incubated with fresh medium and allowed to recover for 24 h for co-immunoprecipitation studies. Otherwise, they were allowed to recover for 6-8 h and re-seeded into 12- well or 24-well dishes and then grown an additional 18 h prior to experimentation.

ERK1/2 Activation and Western Blotting

HEK 293 cells were transiently transfected with the cDNAs described in the *Figure Legends*. 48 h post-transfection cells were serum starved overnight in glutamine-free DMEM and stimulated for the indicated times with 30 μM quisqualate. The cells were then placed on ice, washed 2X with ice-cold phosphate-buffered saline (PBS) and lysed with cold-lysis buffer (50 mM Tris, pH 8.0, 150 mM NaCl, 0.1% Triton X-100) containing protease inhibitors (1 mM AEBSF, 10 μg/ml leupeptin, and 5 μg/ml aprotinin) and phosphatase inhibitors (10 mM NaF, 5 μM Na_3VO_4). The cells were placed on a rocking platform for 15 min at 4°C and centrifuged at 15000 x g for 15 min at 4°C to pellet insoluble material. Cell extracts were solubilized in a 3X SDS sample buffer containing 2-mercaptoethanol (BME). Samples were separated by SDS-PAGE, transferred to a nitrocellulose membrane and immunoblotted to identify phosphorylated (active) and total p42/44 (ERK1/2) (1:1000 dilution, Cell Signaling) followed by a horseradish peroxidase-conjugated secondary anti-rabbit (1:10,000, BioRad). Receptor protein expression was determined by immunoblotting 10 μg of protein from each cell lysate. Proteins were detected using chemiluminescence with the ECL kit from GE Healthcare.

Co-immunoprecipitation

Transfected HEK 293 cells were lysed 48 h post-transfection in cold RIPA buffer (150 mM NaCl, 1% IGEPAL® CA-630, 0.5% sodium deoxycholate, 0.1% SDS, 50 mM Tris pH 8.0; Sigma) plus protease inhibitors (complete EDTA-free; Roche). Cell lysates were sonicated in an

Molecular Pharmacology Fast Forward. Published on January 9, 2013 as DOI: 10.1124/mol.112.081695
This article has not been copyedited and formatted. The final version may differ from this version.

ice water bath for 5 min and then centrifuged at 16,500 x *g* for 20 min at 4°C. A portion of the supernatant was removed and mixed 1:1 with 6X Laemmli sample buffer ("lysate" samples). Anti-FLAG was used to immunoprecipitate ('IP') mGluR1a from resultant lysates. 48 h post-transfection, co-immunoprecipitating proteins and total lysates resolved by SDS–PAGE were immunoblotted (IB) with anti-M2-FLAG-HRP, anti-3F10-HA-HRP or anti-YFP antibodies. Samples were subjected to SDS-PAGE and transferred to nitrocellulose using the iBlot® dry blotting system (Invitrogen). Membranes were blocked in 5% non-fat milk/TBS-T for 1 h at RT. Western blotting was performed using the aforementioned primary antibodies, secondary anti-mouse or -rabbit IgG antibody-HRP conjugates (GE Healthcare), and enhanced chemiluminescence (SuperSignal® West Pico or SuperSignal® West Femto Pierce).

Measurement of inositol phosphate formation

HEK 293 cells were transiently transfected with the cDNAs as described in the *Figure Legends*. 48 h post-transfection cells were incubated overnight in inositol- and glutamine-free DMEM with 100 μCi/ml *myo*-[^{3}H]-Inositol. For all experiments cells were incubated for 1 h in warm HBSS (116 mM NaCl, 20 mM HEPES, 11 mM glucose, 5 mM NaHCO3, 4.7 mM KCl, 2.5 mM CaCl2, 1.2 mM MgSO4, 1.2 mM KH2PO4, pH 7.4) and were then incubated with 10 mM LiCl alone for 10 min followed by 30 μM quisqualate in LiCl for 30 min. Cells were placed on ice and the reaction was stopped with 500 μl of perchloric acid and was neutralized with 400 μl of 0.72 M KOH, 0.6 M $KHCO_3$. Total cellular [^{3}H]-inositol incorporation was determined in 50 μl of cell lysate. Total inositol phosphate was purified by anion exchange chromatography using Dowex 1-X8 (formate form) 200-400 mesh anion exchange resin and [^{3}H]-inositol phosphate formation was determined by liquid scintillation using a Beckman LS 6500 scintillation system.

Confocal microscopy

Confocal microscopy was performed using a Zeiss LSM-510 META laser scanning confocal microscope equipped with a Zeiss 63X, 1.4 numerical aperture, oil immersion lens

Molecular Pharmacology Fast Forward. Published on January 9, 2013 as DOI: 10.1124/mol.112.081695
This article has not been copyedited and formatted. The final version may differ from this version.

(North York, ON, Canada). For live cell imaging, HEK 293 cells expressing FLAG-mGluR1a constructs were serum starved for 1 h at 37°C in HBSS. HEK 293 cells were pre-labelled with Zenon Alexa Fluor 568-conjugated with anti-FLAG polyclonal rabbit antibody (Invitrogen). Cells were then either kept on ice or stimulated with 30 μM quisqualate for 30 min at 37°C. For fixed cell imaging, cells were washed three times at room temperature PBS, fixed for 10 min at room temperature with Periodate-Lysine-Paraformaldehyde (PLP) fixative (McLean and Nakone, 1974) followed by 10 min permeablilization with 0.01% Triton X-100. Cells were blocked with 3% normal donkey serum (Jackson ImmunoResearch) and labelled with rabbit anti-FLAG polyclonal rabbit antibody followed by donkey anti-rabbit Alexa Fluor 488. Endoplasmic reticulum was labelled with red fluorescence protein (GFP)-fused lysine-aspartate-glutamate-leucine (KDEL-GFP) ER retention sequence. Colocalization studies were performed using dual excitation (488, 543 nm) and emission (band pass 505-530 nm and long pass 560 nm for Alexa Fluor 488 and 568, respectively) filter sets.

Flow Cytometry

HEK 293 cells were transiently transfected with the cDNAs described in the *Figure Legends*. 48 h post-transfection cells were placed on ice and washed in ice-cold HBSS. FLAG-tagged mGluR1α constructs were labelled with primary rabbit anti-FLAG antibody (1:500) followed by secondary goat anti-rabbit AlexaFluor-488 antibody (1:500). Cells were incubated for 10 min in 5 mM EDTA, gently removed from dish by pipetting and fixed in 3.6% formaldehyde. Cell surface mean fluorescence was assessed by flow cytometry.

Statistical Analysis

Densitometric data were normalized first for protein expression and the maximum value was set to 100, with all other values displayed as percentage thereof. One-way analysis of variance test (ANOVA) was performed to determine significance, followed by a post-hoc Tukey multiple comparison test or Bonferroni's multiple comparisons test to determine which means

Molecular Pharmacology Fast Forward. Published on January 9, 2013 as DOI: 10.1124/mol.112.081695
This article has not been copyedited and formatted. The final version may differ from this version.

were significantly different ($p < 0.05$) from one another.

Molecular Pharmacology Fast Forward. Published on January 9, 2013 as DOI: 10.1124/mol.112.081695
This article has not been copyedited and formatted. The final version may differ from this version.

RESULTS

Mutations in the cysteine-rich domain alter receptor cell surface expression

Eight somatic variants in *GRM1* were previously identified in variety of tumour types with four localized to the amino-terminal domain of mGluR1a (D44E, A168V, R375G and G396V), three localized to the mGluR1a second intracellular loop (R684C, G688V and R696W), and one localized to the Homer binding motif (P1148L) (Fig. 1) (Kan et al., 2010; Parsons et al., 2008; Sjoblom et al., 2006; Wood et al., 2007). We first examined whether the cell surface expression of FLAG-mGluR1a was affected by each of the mutations introduced into the coding sequence of mGluR1a. None of the somatic mutations resulted in an overall change in cellular protein expression as determined by Western blot (Fig. 2A). Densitometric analysis reveal no differences in total expression of each of the Flag-mGluR1a variants when compared to wild-type FLAG-mGluR1a expression (Fig. 2B). However, FLAG-mGluR1a-R375G and -G396V exhibited reduced cell surface expression as assessed by flow cytometry, with cell surface expression reduced to 39.7 ± 5.1% and 43.4 ± 3.2% of wild type mGluR1a control transfected cells, respectively (Fig. 2C). The reduction in cell surface FLAG-mGluR1a-R375G and -G396V expression was associated with an increased retention of both receptor mutants in the ER as demonstrated by increased colocalization with the ER marker construct KDEL-GFP (Fig. 3D, E). Thus, both the R375G and G396V mutations result in a significant reduction of mGluR1a expression at the cell surface as a consequence of ER retention.

Mutations in the amino-terminus exhibit altered basal and agonist-activated activity

Group I mGluRs activate both IP and ERK signal transduction cascades and exhibit high basal activity (Dale et al., 2000). Interestingly, three of the four amino-terminal mGluR1a variants we examined (A168V, R375G, G396V) showed significantly reduced basal IP formation (in the absence of agonist) compared to wild type, and FLAG-mGluR1a-R375G exhibited basal IP

Molecular Pharmacology Fast Forward. Published on January 9, 2013 as DOI: 10.1124/mol.112.081695
This article has not been copyedited and formatted. The final version may differ from this version.

formation that was indistinguishable from non-transfected cells (Fig. 4A). Quisqualate-mediated activation of FLAG-mGluR1a-A168V (a variant located within the glutamate binding region) resulted in a 63 ± 17% increase in IP formation above basal when compared to control FLAG-mGluR1a transfected cells (Fig. 4B). Quisqualate-stimulated FLAG-mGluR1a-R375G IP formation above basal was comparable to FLAG-mGluR1a wild type transfected cells, despite reduced cell surface expression. However, when total quisqualate-stimulated mGluR1a variant IP formation was assessed, total FLAG-mGluR1a-A168V-stimulated IP formation was indistinguishable from Flag-mGluR1a, whereas total FLAG-mGluR1a-R375G-mediated IP formation was impaired (Fig. 4C). Interestingly, in response to 100 μM glutamate treatment, FLAG-mGluR1a-R375G-mediated IP formation above basal IP levels was reduced to 29 ± 4% of cells transfected with FLAG-mGluR1a (Fig. 4D). Glutamate-mediated activation of FLAG-mGluR1a-A168V also resulted in increased IP formation above basal when compared to control FLAG-mGluR1a transfected cells (Fig. 4D). In response to glutamate, the maximal capacity of FLAG-mGluR1a-A168V to activate G protein signalling was not different from wild type FLAG-mGluR1a, whereas FLAG-mGluR1a-R375G signalling was impaired (Fig. 4E). Therefore, activation of this mutant by glutamate and quisqualate resulted in divergent signalling patterns.

To further evaluate how mutations in the amino terminus affect agonist activation, we looked at dose-dependent receptor activation in response to increasing concentrations of quisqualate. The FLAG-mGluR1a-A168V mutant did not exhibit an alteration in the EC_{50} for quisqualate-mediated IP formation but significantly increased the E_{MAX} for quisqualate-stimulated IP formation (Fig. 5). Interestingly, although FLAG-mGluR1a-R375G maximal response to quisqualate was unchanged from wild type, this mutant produced a significantly right-shifted EC_{50} of 3.1×10^{-6} M compared to wild type EC_{50} of 2.3×10^{-8} M (Fig. 5). Therefore, although FLAG-mGluR1a-R375G couples effectively to the cognate G protein to trigger signal

Molecular Pharmacology Fast Forward. Published on January 9, 2013 as DOI: 10.1124/mol.112.081695
This article has not been copyedited and formatted. The final version may differ from this version.

transduction, this mutant exhibits decreased affinity for the ligand compared to wild type receptor.

R375G displays functional selectivity toward ERK1/2

To examine whether the mGluR1a cancer mutations also affected other mGluR1a-activated cell signalling pathways, we examined whether the variants influenced the ability of mGluR1a to stimulate ERK1/2 phosphorylation in HEK 293 cells. Similar to what we found for IP formation, all four amino-terminal mutations as well as the G688V mutant exhibited decreased basal ERK1/2 phosphorylation, but still displayed a statistically significant increase in IP formation in response to quisqualate treatment (Fig. 6A). Interestingly, although FLAG-mGluR1a-R375G demonstrated decreased basal ERK1/2 phosphorylation, quisqualate treatment of FLAG-mGluR1a-R375G expressing cells resulted in significantly increased ERK1/2 phosphorylation following 1, 5 and 15 min agonist stimulation when compared to wild type FLAG-mGluR1a (Fig. 6B). In contrast, ERK1/2 phosphorylation in response to the activation of either FLAG-mGluR1a-R696W or -P1148L was significantly reduced when compared to wild type FLAG-mGluR1a. Therefore, the R375G mutant appeared to be biased towards the activation of the ERK1/2 pathway, whereas the R696W and P1148L were biased for G protein-mediated signalling. To determine if this altered ERK1/2 activity resulted from differential association with proteins known to mediate mGluR1a activation of ERK, we performed co-immunoprecipitation experiments with the mGluR1a effector Pyk2. When normalized for HA-Pyk2 protein expression, none of the mutants studied exhibited altered association with HA-Pyk2 when compared to wild type FLAG-mGluR1a (Fig. 7). Therefore, the altered downstream activation of ERK1/2 by several of the mutants studied is not mediated by altered receptor association with Pyk2.

Molecular Pharmacology Fast Forward. Published on January 9, 2013 as DOI: 10.1124/mol.112.081695
This article has not been copyedited and formatted. The final version may differ from this version.

GRK2 binding to mGluR1a SNV mutants

Several of the identified mGluR1a alterations are localized to the second intracellular loop domain of the receptor, including R684C, G688V and R696W, a domain that is important for GRK2 binding and phosphorylation-independent desensitization of the receptor (Pin et al., 1994; Dhami et al., 2004). To examine whether GRK2-mediated IP desensitization was altered, we compared the ability of GRK2 to desensitize cells expressing wild type mGluR1a versus the mGluR1a variants. Surprisingly, we observed no alterations in IP formation between cells expressing wild type mGluR1a versus the cancer variants (Fig. 8A), and this was further supported by comparable association between mGluR1a wild type and variants with GRK2 in co-immunoprecipitation studies (Fig. 8B). Therefore, although there are mutations in a region critical for association and desensitization of the receptor by GRK2, we observed neither changes in GRK2-mediated IP desensitization (Fig. 8A) nor decreases in GRK2 interaction between the mGluR1a variants (Fig. 8C).

Attenuated Homer binding to FLAG-mGluR1a P1148L

The carboxyl-terminus mGluR1a encodes a Homer binding motif and the association of Homers with mGluR1a was shown to modulate both the subcellular localization and signalling of mGluR1a (Brakeman et al., 1997; Kammermeier, 2008; Roche et al., 1999, Ango et al., 2002). The introduction of the P1148L variant into the C-tail of FLAG-mGluR1a did not affect IP formation in response to agonist activation of the receptor (Fig. 4), but diminished agonist-stimulated ERK1/2 phosphorylation and resulted in a loss of Homer1b binding to the receptor as determined by co-immunoprecipitation (Fig. 6B and Fig. 9). Homer1b binding to FLAG-mGluR1a-G396V, which was retained in the ER, was also reduced (Fig. 9). The P1148L mutation also resulted in altered subcellular localization of mGluR1a to membrane ruffles in HEK 293 and increased filopodia formation in HEK 293 cells (Fig. 10A-C) and NIH 3TC cells (data not shown). Upon observing the increased filopodia in HEK 293 cells we evaluated this in NIH 3T3

Molecular Pharmacology Fast Forward. Published on January 9, 2013 as DOI: 10.1124/mol.112.081695
This article has not been copyedited and formatted. The final version may differ from this version.

cells; a cell type with more well-characterized morphological changes that are easily quantifiable. As was seen in HEK 293 cells, FLAG-mGluR1a P1148L expression in NIH 3T3 cells also resulted in significantly higher filipodia formation, an effect that was not observed for the wild type receptor (Fig. 10D). Therefore, a loss of homer binding results in increased filipodia formation that might be associated with alterations in cellular migration in an appropriate cancer cell line.

Molecular Pharmacology Fast Forward. Published on January 9, 2013 as DOI: 10.1124/mol.112.081695
This article has not been copyedited and formatted. The final version may differ from this version.

DISCUSSION

In the present study, we have characterised the intracellular localization, signalling, association with regulatory molecules and cellular morphology of eight previously unstudied somatic variants in *GRM1* (Kan et al., 2010; Parsons et al., 2008; Sjoblom et al., 2006; Wood et al., 2007). Group I mGluRs exhibit significant basal G protein activation (Dale et al., 2000). However, three amino-terminal mGluR1a variants, A168V, R375G and G396V, as well as one second intracellular loop variant (G688V) exhibited a loss of basal activity in HEK 293 cells. The reduction in basal activity for the amino-terminal mGluR1a mutations may be the consequence of altered affinity for glutamate that may be released from the HEK 293 cells to feedback on the receptor. However, inconsistent with this notion is the observation that the mGluR1a-A168V mutant exhibits increased activation of IP formation in response to agonist treatment. The intracellular loop mutation G688V also resulted in decreased basal mGluR1a activity without affecting agonist-stimulated responses. The rationale for this observed reduction in basal activity of the mGluR1a-G688V variant remains to be determined.

It is well established that mGluRs activate downstream mitogenic pathways such as the ERK1/2 signaling cascade that contribute to alterations in cell proliferation (Rozengurt, 2007). Group I mGluRs activate ERK1/2 in both calcium-dependent and -independent manners, the latter involving Gβγ and non-receptor tyrosine kinases such as Src and Pyk2 as well as Homer (Nicodemo et al., 2010; Mao et al., 2005). We have identified three mGluR1a mutants with altered ERK1/2 activation. The R696W and P1148L mutations result in a loss of mGluR1a agonist-stimulated ERK1/2 phosphorylation without affecting G protein-coupling required for IP formation. The R375G mutation significantly impairs mGluR1a-mediated IP formation in response to glutamate treatment, and results in an overall reduction in the ability of mGluR1a to stimulate IP formation in response to quisqualate treatment. However, despite the reduced expression of the R375G mutant at the cell surface and decreased overall G protein coupling,

Molecular Pharmacology Fast Forward. Published on January 9, 2013 as DOI: 10.1124/mol.112.081695
This article has not been copyedited and formatted. The final version may differ from this version.

the mutant exhibits enhanced coupling to the activation of ERK1/2 when compared with the wild type mGluR1a, potentially through its ability to signalling via Pyk2. Taken together, these observations suggest that the R375G mutation localized to the amino-terminal domain of mGluR1a may bias receptor signalling via the ERK1/2 pathway, which may be relevant to a cancer phenotype.

The overexpression of mGluR1 in melanocytes promotes development and growth of melanoma (Polluck et al., 2003; Ohtani et al., 2008; Martino et al., 2012), and more recently, the molecular mechanisms supporting mGluR1-promoted melanoma formation have been elucidated. Although it appears that activation of numerous mGluR1-promoted signalling pathways is required for melanoma development, it is activation of the ERK pathway by mGluR1 that plays a key role in melanoma growth (Abdel-Daim et al., 2010); as such, mGluR1 R375G which biases receptor signalling to ERK may promote tumor progression through increased cancer growth.

Receptor modulation by regulatory proteins such as GRK2 represents a major mechanism controlling the magnitude and duration of GPCR signal transduction. GRK2-mediated attenuation of mGluR1a signalling occurs as the consequence of the concomitant association of the kinase with the second intracellular loop domain of the receptor and Gαq (Dhami et al., 2004; Dhami et al., 2005; Dhami and Ferguson, 2006; Ferguson, 2007). We investigated here the effect of three intracellular loop 2 SNVs on the association of GRK2 with mGluR1a. We found that all the mutations retained GRK2 association. In line with this, GRK2 overexpression resulted in normal attenuation of G protein signalling in response to the activation of all the mGluR1a mutants. Interestingly, we found that ERK1/2 activation in response to activation of mGluR1a-R696W is lost, suggesting that this residue may contribute to the regulation of ERK1/2 signalling by the receptor. Our previous studies have shown that Pyk2 binds to the second intracellular loop domain of mGluR1a and may directly contribute to the

Molecular Pharmacology Fast Forward. Published on January 9, 2013 as DOI: 10.1124/mol.112.081695
This article has not been copyedited and formatted. The final version may differ from this version.

activation of ERK1/2 (Nicodemo et al., 2010). However, here we find that none of the mutants studied show altered association with Pyk2.

Of the many regulatory proteins that interact with Group I mGluRs, the Homer family of proteins are predominantly featured as they are synaptically localized and couple Group I mGluRs to the activation of a variety of ion channels at the synapse (Ango et al., 2002; Roche et al., 1999; Tadokoro et al., 1999). Here we show that the mGluR1a variant P1148L does not associate with Homer1b, is uncoupled from the activation of ERK1/2 and causes enhanced filopodia formation in HEK 293 cells. The loss of agonist-stimulated ERK1/2 phosphorylation by the mGluR1a-P1148L mutant is consistent with recent reports that Homer1a may contribute in part to the coupling of mGluR1a to the activation of ERK1/2 (Mao et al., 2005). The mechanism by which the P1148L mutation leads to increased filopodia formation is unclear, but Homer proteins may contribute to the regulation of actin dynamics through their interactions with the actin cytoskeletal regulatory proteins Cdc42 and Drebin (Shiraishi-Yamaguchi et al., 2009).

There are several factors involved in tumor progression and metastasis, including altered cell motility and promotion of angiogenesis. Numerous GPCRs have been shown to drive cell migration and vascular remodelling through both direct and indirect mechanism, including PAR and AT1R. Recently, CCK2R cancer variants were shown to alter cellular morphology (*i.e.*, filopodia and lamellipodia formation), increase cell migration, and promote angiogenesis, leading to enhanced tumorigenesis (Willard et al., 2012). Ectopic overexpression of mGluR1 in both melanocytes and epithelial cells promotes formation of robust tumours, and the malignancy of these tumours is evident by increased angiogenesis and invasion to muscle and intestine (Shin et al., 2008; Martino et al., 2012). Thus, mGluR1 P1148L which increases filopodia formation may stimulate tumorigenesis through changes in cell behaviour that promote a malignant phenotype.

In conclusion, in this study, we characterized the signalling and intracellular localization of eight somatic mutations in *GRM1* identified in genome-wide screens of various cancer types.

Molecular Pharmacology Fast Forward. Published on January 9, 2013 as DOI: 10.1124/mol.112.081695
This article has not been copyedited and formatted. The final version may differ from this version.

We identified two mutations involved in plasma membrane targeting as well as several mutations differentially affecting IP formation and MAPK signalling of this receptor. For example, we demonstrate that the R375G SNV preferentially couples to ERK1/2 activation while exhibiting decreased basal and glutamate-activated inositol phosphate production. Additionally, the A168V SNV displays decreased basal and increased agonist-mediated IP formation. These alterations in the mGluR1a activity may contribute, at least in part, to the phenotype of the cancer in which they were identified. This study sheds new light on the functionality of different regions of the receptor as well as further defining the residues involved in mGluR1a signalling and the role of mGluR1a signalling in pathologies and may provide an exciting opportunity for developing new mGluR1a-targeted treatments.

ACKNOWLEDGEMENTS – The authors thank James Starling and Christoph Reinhard for project support. We thank Mel Baez, Beverly Heinz, Shaoyou Chu, Christopher Moxham, Shaillay Kumar Dogra, Mohamed Roohul Ameen, Jiahang Song, Dong Liang Guo, Marcio Chedid, Andrew Capen, Yue-wei Qian, Francis Willard, David Clawson and Suzie Chen for experimental assistance and project guidance. SSGF also holds a Tier I Canada Research Chair in Molecular Neurobiology and is a Career Investigator of the Heart and Stroke Foundation of Ontario. JLE is the recipient of an Ontario Graduate Scholarship.

Molecular Pharmacology Fast Forward. Published on January 9, 2013 as DOI: 10.1124/mol.112.081695
This article has not been copyedited and formatted. The final version may differ from this version.

AUTHORSHIP CONTRIBUTIONS

Participated in research design: Esseltine, Willard, Lajiness, Barber, Ferguson

Conducted experiments: Esseltine, Willard, Wulur

Contributed new reagents or analytical tools: Esseltine, Willard, Lajiness, Barber, Ferguson

Performed data analysis: Esseltine, Willard, Wulur

Wrote or contributed to the writing of the manuscript: Esseltine, Willard, Barber, Ferguson

Molecular Pharmacology Fast Forward. Published on January 9, 2013 as DOI: 10.1124/mol.112.081695
This article has not been copyedited and formatted. The final version may differ from this version.

REFERENCES

Abdel-Daim M, Funasaka Y, Komoto M, Nakagawa Y, Yanagita E, Nishigori C (2010) Pharmacogenomics of metabotropic glutamate receptor subtype 1 and in vivo malignant melanoma formation. J Dermatol 37:635-646.

Ango F, Robbe D, Tu JC, Xiao B, Worley P.F, Pin JP, Bockaert J, and Fagni L (2002) Homer-dependent cell surface expression of metabotropic glutamate receptor type 5 in neurons. Mol Cell Neurosci 20:323-329.

Bhattacharya M, Babwah AV, Godin C, Anborgh PH, Dale LB, Poulter MO, and Ferguson SSG (2004) Ral and phospholipase D2-dependent pathway for constitutive metabotropic glutamate receptor endocytosis. J. Neurosci. 24:8752-8761.

Brakeman PR, Lanahan AA, O'Brien R, Roche K, Barnes CA, Huganir RL, and Worley PF (1997) Homer: a protein that selectively binds metabotropic glutamate receptors. Nature 386:284-288.

Choi KY, Chang K, Pickel JM, Badger JD 2nd, Roche KW. (2011) Expression of the metabotropic glutamate receptor 5 (mGluR5) induces melanoma in transgenic mice. Proc Natl Acad Sci U S A 10815219-15224.

Conn PJ, and Pin JP (1997) Pharmacology and functions of metabotropic glutamate receptors. Annu Rev Pharmacol Toxicol 37:205-237.

Dale LB, Babwah AV, Bhattacharya M, Kelvin DJ, and Ferguson SSG (2001) Spatial-temporal patterning of metabotropic glutamate receptor-mediated inositol 1,4,5-triphosphate, calcium, and protein kinase C oscillations: protein kinase C-dependent receptor

phosphorylation is not required. J Biol Chem 276:35900-35908.

Dale LB, Bhattacharya M, Anborgh PH, Murdoch B, Bhatia M, Nakanishi S, and Ferguson SSG (2000) G protein-coupled receptor kinase-mediated desensitization of metabotropic glutamate receptor 1A protects against cell death. J Biol Chem 275:38213-38220.

Dhami GK, and Ferguson SSG (2006) Regulation of metabotropic glutamate receptor signaling, desensitization and endocytosis. Pharmacol Ther 111:260-271.

Dhami GK, Babwah AV, Sterne-Marr R, and Ferguson SSG (2005) Phosphorylation-independent regulation of metabotropic glutamate receptor 1 signaling requires g protein-coupled receptor kinase 2 binding to the second intracellular loop. J Biol Chem 280:24420-24427.

Dhami GK, Dale LB, Anborgh PH, O'Connor-Halligan KE, Sterne-Marr R, and Ferguson SSG (2004) G Protein-coupled receptor kinase 2 regulator of G protein signaling homology domain binds to both metabotropic glutamate receptor 1a and Galphaq to attenuate signaling. J Biol Chem 279:16614-16620.

Dingledine R, Borges K, Bowie D, and Traynelis SF (1999) The glutamate receptor ion channels. Pharmacol Rev 51:7-61.

Emery AC, Pshenichkin S, Takoudjou GR, Grajkowska E, Wolfe BB, Wroblewski JT (2010) The protective signaling of metabotropic glutamate receptor 1 Is mediated by sustained, beta-arrestin-1-dependent ERK phosphorylation. J Biol Chem 285:26041-8.

Ferguson SSG (2007) Phosphorylation-independent attenuation of GPCR signaling. Trends Pharmacol Sci 28:173-179.

Francesconi A, Duvoisin RM (2000) Opposing effects of protein kinase C and protein kinase A on metabotropic glutamate receptor signaling: selective desensitization of the inositol trisphosphate/Ca2+ pathway by phosphorylation of the receptor-G protein-coupling domain. Proc Natl Acad Sci U S A 97:6185-90.

Francesconi A, and Duvoisin RM (1998) Role of the second and third intracellular loops of metabotropic glutamate receptors in mediating dual signal transduction activation. J Biol Chem 273:5615-5624.

Huang S, Cao J, Jiang M, Labesse G, Liu J, Pin JP, Rondard P (2011) Interdomain movements in metabotropic glutamate receptor activation. Proc Natl Acad Sci U S A 108:15480-5.

Kammermeier PJ (2008) Endogenous homer proteins regulate metabotropic glutamate receptor signaling in neurons. J Neurosci 28:8560-7.

Kan Z, Jaiswal BS, Stinson J, Janakiraman V, Bhatt D, Stern HM, Yue P, Haverty PM, Bourgon R, Zheng J, (2010) Diverse somatic mutation patterns and pathway alterations in human cancers. Nature 466:869-873.

Krupnick JG, and Benovic JL (1998) The role of receptor kinases and arrestins in G protein-coupled receptor regulation. Annu Rev Pharmacol Toxicol 38:289-319.

Mao L, Yang L, Tang Q, Samdani S, Zhang G, and Wang JQ (2005) The scaffold protein Homer1b/c links metabotropic glutamate receptor 5 to extracellular signal-regulated protein kinase cascades in neurons. J Neurosci 25:2741-2752.

Martino JJ, Wall BA, Mastrantoni E, Wilimczyk BJ, La Cava SN, Degenhardt K, White E, Chen S. (2013) Metabotropic glutamate receptor 1 (Grm1) is an oncogene in epithelial cells.

Oncogene. 2012 Oct 22. doi: 10.1038/onc.2012.471. [Epub ahead of print]

Mundell SJ, Pula G, Carswell K, Roberts PJ, and Kelly E (2003) Agonist-induced internalization of metabotropic glutamate receptor 1A: structural determinants for protein kinase C- and G protein-coupled receptor kinase-mediated internalization. J Neurochem 84:294-304.

Mundell SJ, Pula G, McIlhinney RA, Roberts PJ, and Kelly E (2004) Desensitization and internalization of metabotropic glutamate receptor 1a following activation of heterologous Gq/11-coupled receptors. Biochemistry 43:7541-7551.

Nicodemo AA, Pampillo M, Ferreira LT, Dale LB, Cregan T, Ribeiro FM, and Ferguson SSG (2010) Pyk2 uncouples metabotropic glutamate receptor G protein signaling but facilitates ERK1/2 activation. Mol Brain 3:4.

Niswender CM, and Conn PJ (2010) Metabotropic glutamate receptors: physiology, pharmacology, and disease. Annu Rev Pharmacol Toxicol 50:295-322.

O'Hara PJ, Sheppard PO, Thøgersen H, Venezia D, Haldeman BA, McGrane V, Houamed KM, Thomsen C, Gilbert TL, Mulvihill ER (1993) The ligand-binding domain in metabotropic glutamate receptors is related to bacterial periplasmic binding proteins. Neuron 11:41-52.

Ohtani Y, Harada T, Funasaka Y, Nakao K, Takahara C, Abdel-Daim M, Sakai N, Saito N, Nishigori C, Aiba A (2008) Metabotropic glutamate receptor subtype-1 is essential for in vivo growth of melanoma.Oncogene 27:7162-7170.

Olney JW (1994) Excitatory transmitter neurotoxicity. Neurobiol Aging 15:259-260.

Parsons DW, Jones S, Zhang X, Lin JC, Leary RJ, Angenendt P, Mankoo P, Carter H, Siu

IM, Gallia GL, (2008) An integrated genomic analysis of human glioblastoma multiforme. Science 321:1807-1812.

Pin JP, Galvez T, and Prezeau L (2003) Evolution, structure, and activation mechanism of family 3/C G-protein-coupled receptors. Pharmacol Ther 98:325-354.

Pin JP, Kniazeff J, Binet V, Liu J, Maurel D, Galvez T, Duthey B, Havlickova M, Blahos J, Prezeau L, and Rondard P (2004) Activation mechanism of the heterodimeric GABA(B) receptor. Biochem Pharmacol 68:1565-1572.

Pollock PM, Cohen-Solal K, Sood R, Namkoong J, Martino JJ, Koganti A, Zhu H, Robbins C, Makalowska I, Shin SS, Marin Y, Roberts KG, Yudt LM, Chen A, Cheng J, Incao A, Pinkett HW, Graham CL, Dunn K, Crespo-Carbone SM, Mackason KR, Ryan KB, Sinsimer D, Goydos J, Reuhl KR, Eckhaus M, Meltzer PS, Pavan WJ, Trent JM, Chen S. (2003) Melanoma mouse model implicates metabotropic glutamate signaling in melanocytic neoplasia. Nat Genet. 34:108-112.

Prickett TD, Wei X, Cardenas-Navia I, Teer JK, Lin JC, Walia V, Gartner J, Jiang J, Cherukuri PF, Molinolo A, Davies MA, Gershenwald JE, Stemke-Hale K, Rosenberg SA, Margulies EH, Samuels Y (2011) Exon capture analysis of G protein-coupled receptors identifies activating mutations in GRM3 in melanoma. Nat Genet 43:1119-1126.

Ribeiro FM, Ferreira LT, Paquet M, Cregan T, Ding Q, Gros R and Ferguson SSG (2009) Phosphorylation-independent regulation of metabotropic glutamate receptor 5 desensitization and internalization by G protein-coupled receptor kinase 2 in striatal neurons. J Biol Chem 284: 23444-23453.

Roche KW, Tu JC, Petralia RS, Xiao B, Wenthold RJ, and Worley PF (1999) Homer 1b

regulates the trafficking of group I metabotropic glutamate receptors. J Biol Chem 274:25953-25957.

Romano C, Yang WL, O'Malley KL (1996) Metabotropic glutamate receptor 5 is a disulfide-linked dimer. J Biol Chem 271:28612-6.

Rozengurt E (2007) Mitogenic signaling pathways induced by G protein-coupled receptors. J Cell Physiol 213:589-602.

Schoepp DD, and Johnson BG (1988) Selective inhibition of excitatory amino acid-stimulated phosphoinositide hydrolysis in the rat hippocampus by activation of protein kinase C. Biochem Pharmacol 37:4299-4305.

Shin SS, Namkoong J, Wall BA, Gleason R, Lee HJ, Chen S (2008) Oncogenic activities of metabotropic glutamate receptor 1 (Grm1) in melanocyte transformation. Pigment Cell Melanoma Res 21:368-378.

Shiraishi-Yamaguchi Y, Furuichi T (2007) The Homer family proteins. Genome Biol 8:206.

Shiraishi-Yamaguchi Y, Sato Y, Sakai R, Mizutani A, Knöpfel T, Mori N, Mikoshiba K, Furuichi T. (2009) Interaction of Cupidin/Homer2 with two actin cytoskeletal regulators, Cdc42 small GTPase and Drebrin, in dendritic spines. BMC Neurosci 10:25.

Sjoblom T, Jones S, Wood LD, Parsons DW, Lin J, Barber TD, Mandelker D, Leary RJ, Ptak J, Silliman N, et al. (2006) The consensus coding sequences of human breast and colorectal cancers. Science 314:268-274.

Speyer CL, Smith JS, Banda M, DeVries JA, Mekani T, Gorski DH (2012) Metabotropic glutamate receptor-1: a potential therapeutic target for the treatment of breast cancer. Breast

Cancer Res Treat 132:565-573.

Tadokoro S, Tachibana T, ImanakaT, Nishida W, and Sobue K (1999) Involvement of unique leucine-zipper motif of PSD-Zip45 (Homer 1c/vesl-1L) in group 1 metabotropic glutamate receptor clustering. Proc Natl Acad Sci U S A 96:13801-13806.

Thandi S, Blank JL, Challiss RA (2002) Group-I metabotropic glutamate receptors, mGlu1a and mGlu5a, couple to extracellular signal-regulated kinase (ERK) activation via distinct, but overlapping, signaling pathways. J Neurochem 83:1139-53.

Tu JC, Xiao B, Yuan JP, Lanahan AA, Leoffert K, Li M, Linden DJ, Worley PF (1998) Homer binds a novel proline-rich motif and links group 1 metabotropic glutamate receptors with IP receptors. Neuron 21:717-26.

Wang M, Bianchi R, ChuangSC, Zhao W, and Wong RK (2007) Group I metabotropic glutamate receptor-dependent TRPC channel trafficking in hippocampal neurons. J Neurochem 101:411-421.

Willard MD, Lajiness ME, Wulur IH, Feng B, Swearingen ML, Uhlik MT, Kinzler KW, Velculescu VE, Sjöblom T, Markowitz SD, Powell SM, Vogelstein B, Barber TD (2012) Somatic mutations in CCK2R alter receptor activity that promote oncogenic phenotypes. Mol Cancer Res. 10:739-749.

Molecular Pharmacology Fast Forward. Published on January 9, 2013 as DOI: 10.1124/mol.112.081695
This article has not been copyedited and formatted. The final version may differ from this version.

FOOTNOTES

This work was supported by an operating grant from the Canadian Institutes of Health Research (CIHR) [MOP-111093]. JLE and MDW contributed equally to this work.

Molecular Pharmacology Fast Forward. Published on January 9, 2013 as DOI: 10.1124/mol.112.081695
This article has not been copyedited and formatted. The final version may differ from this version.

FIGURE LEGENDS

Figure 1: **Eight somatic variants in *GRM1* (mGluR1a) found in cancer**

Location of eight somatic mutations have been identified within the coding sequence for mGluR1a including: A168V, a mutation in the orthosteric glutamate binding region identified in lung adenocarcinoma; two mGluR1a variants in the cysteine-rich region, R375G (identified in squamous cell carcinoma) and G396V (identified in lung adenocarcinoma); three variants in the second intracellular loop including: the glioblastoma mutation, R684C, the squamous cell carcinoma mutation, G688V, and the colorectal cancer R696W mutation located close to the putative PKC phosphorylation site T695A. An additional colorectal cancer mutation is located within the Homer binding region in the carboxyl-terminal region of mGluR1a, P1148L.

Figure 2: **Cell surface expression and intracellular localization of mGluR1a variants. (A)** Representative western blot of HEK 293 cells transfected with 1-3.5 μg of plasmid cDNA encoding FLAG-tagged mGluR1a SNV constructs. **(B)** Shown is the densitometric analysis of autoradiographs showing the mean ± SEM of five independent experiments examining the total cellular expression of wild-type FLAG-mGluR1a and the FLAG-mGluR1a variants. **(C)** HEK 293 cells transfected with 2 μg of plasmid cDNA encoding FLAG-tagged mGluR1a SNV constructs were immunolabelled and cell surface mean fluorescence was assessed by flow cytometry. Data were normalized for total cell surface wild type mGluR1a protein expression. Data represents the mean ± SD of four independent experiments. *, $p < 0.05$ compared with wild type mGluR1a expression.

Figure 3: **mGluR1a variants localize to endoplasmic reticulum.** Representative confocal micrographs illustrating receptor intracellular localization (red) and co-localization with the endoplasmic reticulum marker GFP-KDEL (green). HEK 293 cells transfected with 1-3.5 μg of

Molecular Pharmacology Fast Forward. Published on January 9, 2013 as DOI: 10.1124/mol.112.081695
This article has not been copyedited and formatted. The final version may differ from this version.

plasmid cDNA encoding either **(A)** FLAG-tagged mGluR1a, **(B)** FLAG-tagged mGluR1a-D44E, (C) FLAG-tagged mGluR1a-A168V, **(D)** FLAG-tagged mGluR1a-R375G, or **(E)** FLAG-tagged mGluR1a-G396V constructs along with 1 μg of plasmid cDNA encoding KDEL-GFP were fixed and immunolabelled for total cellular compliment of receptor. Images are representative of 3 independent experiments. Bars represent 10 μm.

Figure 4: **Mutations in mGluR1a alter basal and agonist-activated inositol phosphate formation.** HEK 293 cells transiently transfected with 1-3.5 μg of plasmid cDNA encoding FLAG-tagged mGluR1a SNV constructs. **(A)** Basal IP formation was determined in cells that were labelled overnight with *myo*-(^{3}H)Inositol in glutamine-free DMEM and incubated for 10 min with 10 mM LiCl. **(B)** Increase in IP formation above basal following agonist stimulation with 30 μM quisqualate for 30 min. **(C)** Total IP formation (basal + agonist stimulated) following agonist stimulation with 30 μM quisqualate. **(D)** Increase in IP formation above basal following agonist stimulation with 100 μM glutamate for 30 min. **(E)** Total IP formation (basal + agonist stimulated) following agonist stimulation with 100 μM glutamate. Data were normalized for mGluR1 protein expression at the cell surface as determined by flow cytometry and represent the mean ± SD of four independent experiments. *, $p < 0.05$ compared to wild type mGluR1a IP formation.

Figure 5: **Mutations in mGluR1a alter dose-dependent quisqualate inositol phosphate formation.** HEK 293 cells transiently transfected with 2-3.5 μg of plasmid cDNA encoding FLAG-tagged mGluR1a amino-terminal mutant constructs. Increases in IP formation above basal was determined in cells labelled overnight with *myo*-(^{3}H)Inositol in glutamine-free DMEM and incubated for 10 min with 10 mM LiCl followed by 30 min in 10 mM LiCl with increasing concentrations of quisqualate. Data were normalized for protein expression and represent the mean ± SD of three independent experiments.

Molecular Pharmacology Fast Forward. Published on January 9, 2013 as DOI: 10.1124/mol.112.081695
This article has not been copyedited and formatted. The final version may differ from this version.

Figure 6: **Mutations in mGluR1a alter agonist-stimulated ERK1/2 activation. (A)** HEK 293 cells were transiently transfected with 2 μg of plasmid cDNA encoding FLAG-mGluR1a SNV constructs. Forty-eight hours post-transfection cells were serum starved overnight in glutamine-free DMEM and stimulated for 15 min with 30 μM quisqualate. Shown are representative immunoblots for phosphorylated and total p42/44 (ERK1/2). The data were normalized for protein expression and plotted as the percent change in ERK1/2 phosphorylation compared to wild type (WT) mGluR1a ERK1/2 phosphorylation on the same immunoblot in the absence of agonist treatment (control). The data represent the mean ± SD of five independent experiments *, $p < 0.05$ compared to basal ERK1/2 phosphorylation. Ψ, $p < 0.05$ compared to agonist-stimulated wild type mGluR1a ERK1/2 phosphorylation. **(B)** HEK 293 cells were transiently transfected with 2 μg of plasmid cDNA encoding FLAG-mGluR1a, FLAG-mGluR1a-R696W, FLAG-mGluR1a-P1148 or FLAG-mGluR1a-R375G. Forty-eight hours post-transfection cells were serum starved overnight in glutamine-free DMEM and stimulated for 0, 1, 5 or 15 min with 30 μM quisqualate. Shown are representative immunoblots for phosphorylated and total p42/44 (ERK1/2). The data represent the mean ± SD of five independent experiments *, $p < 0.05$ compared to basal ERK1/2 phosphorylation. ns, not significant, Ψ, $p < 0.05$ compared to agonist-stimulated wild type mGluR1a ERK1/2 phosphorylation.

Figure 7: **mGluR1a mutants maintain association with Pyk2. (A)** HEK 293 cells were transiently transfected with 2-3.5 μg of plasmid cDNA encoding FLAG-tagged mGluR1a SNV constructs along with 1 μg of plasmid cDNA encoding HA-Pyk2. Forty-eight hours post-transfection, the FLAG-mGluR1a SNV constructs were immunoprecipitated with FLAG antibody and immunoprecipitated protein resolved by SDS–PAGE and immunoblotted with FLAG, and HA antibodies. **(B)** Shown is the densitometric analysis of autoradiographs showing the mean ±

Molecular Pharmacology Fast Forward. Published on January 9, 2013 as DOI: 10.1124/mol.112.081695
This article has not been copyedited and formatted. The final version may differ from this version.

SEM of four independent experiments examining the co-immunoprecipitation of HA-Pyk2 with the FLAG-mGluR1a SNV constructs. The data is normalized for FLAG-mGluR1a and HA-Pyk2 protein expression and presented as a percentage of HA-Pyk2 co-immunoprecipitation with wild type mGluR1a.

Figure 8: **Effect of mGluR1a variants on GRK2 binding and receptor desensitization. (A)** HEK 293 cells were transiently transfected with 2 μg of plasmid cDNA encoding FLAG-tagged mGluR1a SNV constructs along with 1 μg of plasmid cDNA encoding either empty vector or HA-GRK2. Cells were labelled overnight with *myo*-(^{3}H)inositol in glutamine-free DMEM, incubated for 10 min with 10 mM LiCl and then treated with 30 μM quisqualate for 30 min. Data is expressed as the increase in IP formation above basal following agonist stimulation with 30 μM quisqualate for 30 min. Data were normalized for mGluR1 protein expression at the cell surface as determined by flow cytometry and represent mean ± SD of three independent experiments. *, $p < 0.05$ compared to agonist-stimulated IP formation in the absence of GRK2 overexpression. **(B)** Forty-eight hours post-transfection, the FLAG-mGluR1a SNV constructs were immunoprecipitated with FLAG antibody and immunoprecipitated protein resolved by SDS–PAGE and immunoblotted with FLAG, GFP (YFP) and actin antibodies. The blots have been cut to remove lanes that correspond to FLAG-mGluR1a mutants examined that did not correspond to mGluR1a SNVs and were not pursued functionally. **(C)** Shown is the densitometric analysis of autoradiographs showing the mean ± SEM of four independent experiments examining the co-immunoprecipitation of YFP-GRK2 with the FLAG-mGluR1a SNV constructs. The data is normalized for FLAG-mGluR1a and YFP-GRK2 protein expression and presented as a percentage of YFP-GRK2 co-immunoprecipitation with wild type mGluR1a.

Molecular Pharmacology Fast Forward. Published on January 9, 2013 as DOI: 10.1124/mol.112.081695
This article has not been copyedited and formatted. The final version may differ from this version.

Figure 9: **mGluR1a P1148L is deficient in Homer1b binding. (A)** HEK 293 cells were transiently transfected with 2 μg of plasmid cDNA encoding FLAG-tagged mGluR1a SNV constructs along with 1 μg of plasmid cDNA encoding HA-Homer1b. Forty-eight hours post-transfection, the FLAG-mGluR1a SNV constructs were immunoprecipitated with FLAG antibody and immunoprecipitated protein resolved by SDS–PAGE and immunoblotted with FLAG, HA and actin antibodies. The blots have been cut to remove lanes that correspond to FLAG-mGluR1a mutants examined that did not correspond to mGluR1a SNVs and were not pursued functionally. **(B)** Shown is the densitometric analysis of autoradiographs showing the mean ± SD of four independent experiments examining the co-immunoprecipitation of HA-Homer1b with the FLAG-mGluR1a SNV constructs. The data is normalized to HA-Homer1b co-immunoprecipitation with wild type mGluR1a. *, $p < 0.05$ compared to wild type FLAG-mGluR1a.

Figure 10: **Homer binding mutant mGluR1a P1148L promotes filopodia formation.** Representative confocal micrographs illustrating receptor localization and cell morphology in HEK 293 cells transiently transfected with 2 μg of plasmid cDNA encoding either **(A)** wild type FLAG-mGluR1a, or **(B)** FLAG-mGluR1a-P1148L (. Cells were fixed and immunolableled for total cellular mGluR1a expression. Images are representative of three independent experiments. Bars represent 10 μm. **(C)** Graph scoring the number of filipodia per cell. NIH 3T3 cells transiently transfected with 2 μg of plasmid cDNA encoding either FLAG-mGluR1a wild type or FLAG-mGluR1a-P1148L were fixed and immunolabelled for total cellular compliment of the receptor and number of filopodia were counted per field of view by a blinded observer. Filipodia were defined as cellular protrusions. Data represent the mean ± SD of 300 random cells total, 100 from 3 independent experiments.

Molecular Pharmacology Fast Forward. Published on January 9, 2013 as DOI: 10.1124/mol.112.081695
This article has not been copyedited and formatted. The final version may differ from this version.

Table 1. Somatic mutations found in *GRM1* (mGluR1a) in cancers.*Mutations characterized in the manuscript**.**

Protein Change	Type	Location	Cancer Subtype	Reference
S33L	missense	LB	Upper aerodigestive tract, Squamous cell	Durinck *et al*., 2011
*D44E	missense	LB	Lung, Adeno	Kan *et al*., 2010
R71K	missense	LB	Skin, Squamous	Durinck *et al*., 2011
R78H	missense	LB	Ovary, Serous	CGARN, 2011
D87H	missense	LB	Ovary, Serous	CGARN, 2011
A91T	missense	LB	Large intestine, Adeno	TCGA
K153N	missense	LB	Large intestine, Adeno	TCGA
*A168V	missense	LB	Lung, Adeno	Kan *et al*., 2010
A184T	missense	LB	Haematopoietic and lymphoid tissue, Chronic lymphocytic leukaemia-small lymphocytic lymphoma	Quesada *et al*., 2011
W224C	missense	LB	Ovary, Serous	CGARN, 2011
A229S	missense	LB	Ovary, Serous	CGARN, 2011
R275H	missense	LB	Large intestine, Adeno	TCGA
R297	nonsense	LB	Breast, Ductal	-
*R375G	missense	LB	Lung, Squamous cell	Kan *et al*., 2010
E386	nonsense	LB	Lung, Adeno	Kan *et al*., 2010
*G396V	missense	LB	Lung, Adeno	Kan *et al*., 2010
I414V	missense	LB	Large intestine, Adeno	TCGA
P444L	missense	LB	Upper aerodigestive tract, Squamous cell	Stransky *et al*., 2011
C547F	missense	LB	Skin, Squamous	Durinck *et al*., 2011
D619A	missense	il1	Breast, Basal, triple-negative	Shah *et al*., 2012
S626C	missense	il1	CNS, Astrocytoma Grade IV	CGARN, 2008
T655N	missense	ex2	Large intestine, Adeno	TCGA
R661H	missense	ex2	Large intestine, Adeno	TCGA
*R684C	missense	il2	CNS, Astrocytoma Grade IV	Parsons *et al*., 2008
*G688V	missense	il2	Lung, Squamous cell	Kan *et al*., 2010
*R696W	missense	il2	Large intestine, Adeno	Sjöblom *et al*., 2006; Wood *et al*., 2007
Q706	nonsense	il2	Upper aerodigestive tract	Durinck *et al*., 2011
N782I	missense	il3	Large intestine, Adenocarcinoma	TCGA
S783I	missense	il3	Breast, Basal, triple-negative	Shah *et al*., 2012
R967H	missense	C-tail	CNS, Astrocytoma grade IV	CGARN, 2008
E1006K	missense	C-tail	Skin, Squamous	Durinck *et al*., 2011
D1096N	missense	C-tail	Ovary, Serous carcinoma	CGARN, 2011
P1148L	missense	C-tail	Large Intestine, Adeno	Wood *et al*., 2007

Figure 1

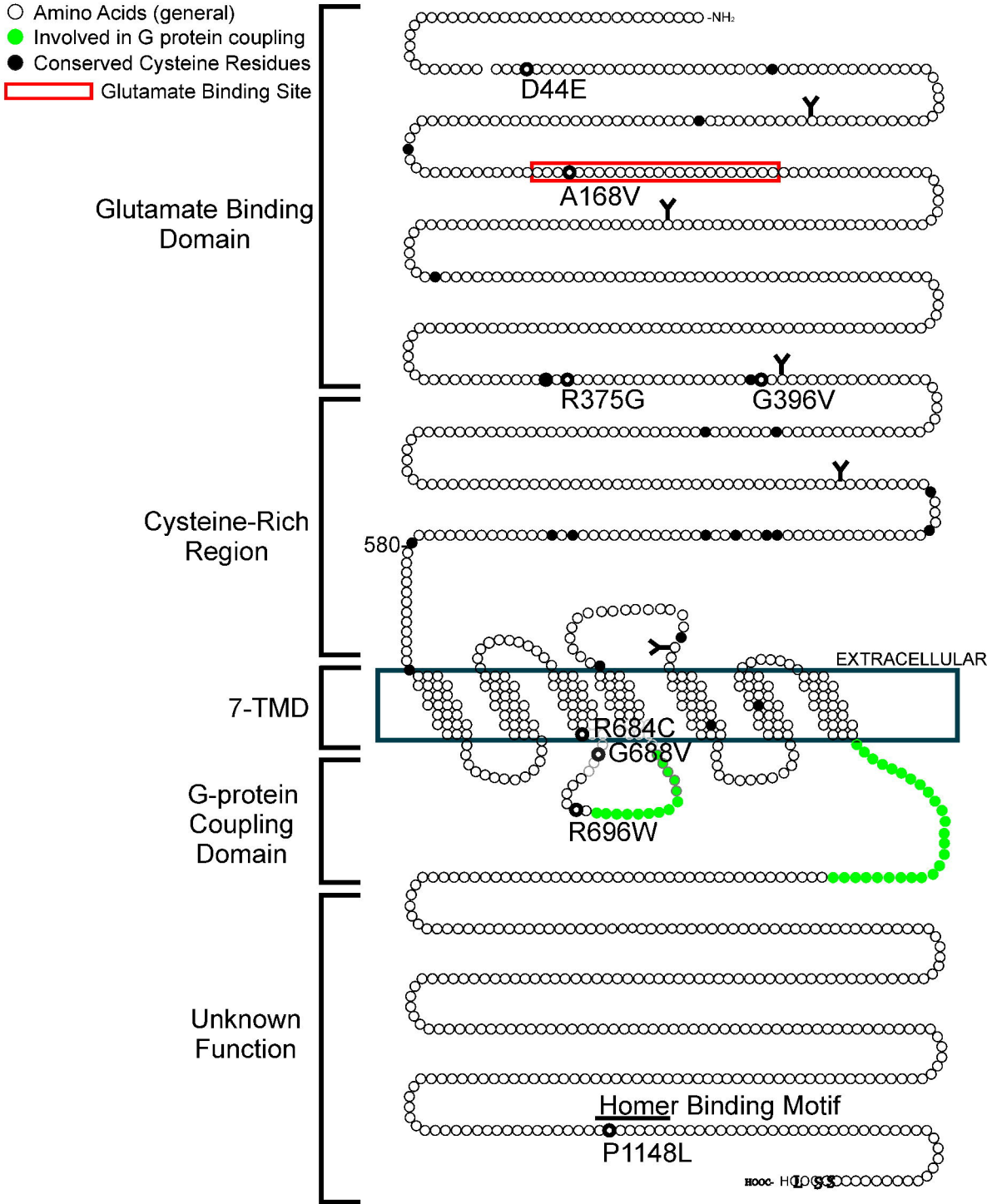
Amino Acids (general)
Involved in G protein coupling
Conserved Cysteine Residues
Glutamate Binding Site
Glutamate Binding Domain
Cysteine-Rich Region
7-TMD
G-protein Coupling Domain
Unknown Function
-NH2
D44E
A168V
R375G
G396V
580
EXTRACELLULAR
R684C
G688V
R696W
Homer Binding Motif
P1148L

Figure 2

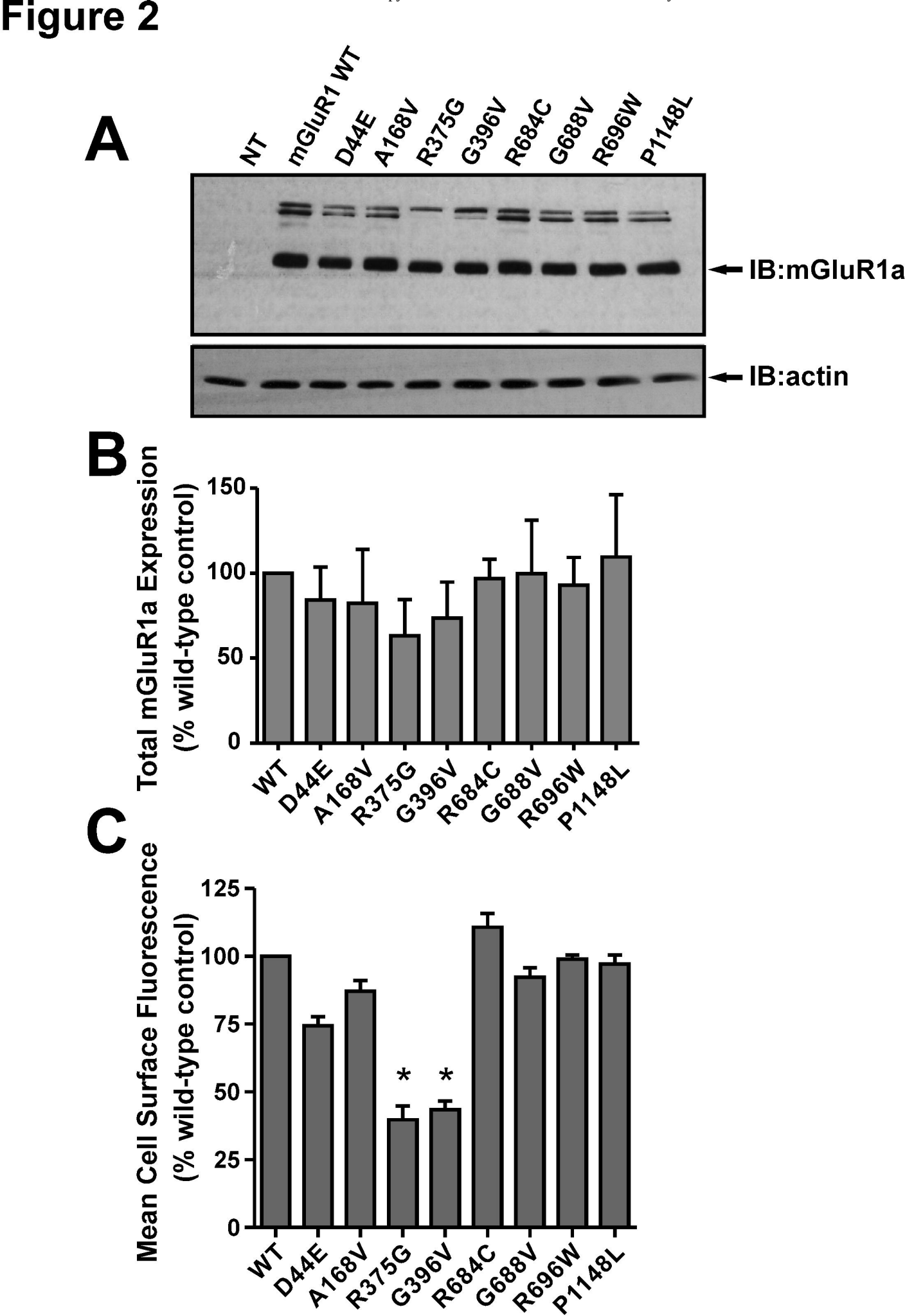
A
NT
mGluR1 WT
D44E
A168V
R375G
G396V
R684C
G688V
R696W
P1148L
IB:mGluR1a
IB:actin
B
Total mGluR1a Expression
(% wild-type control)
150
100
50
0
WT
D44E
A168V
R375G
G396V
R684C
G688V
R696W
P1148L
C
Mean Cell Surface Fluorescence
(% wild-type control)
125
100
75
50
25
0
*
*
WT
D44E
A168V
R375G
G396V
R684C
G688V
R696W
P1148L

Figure 3

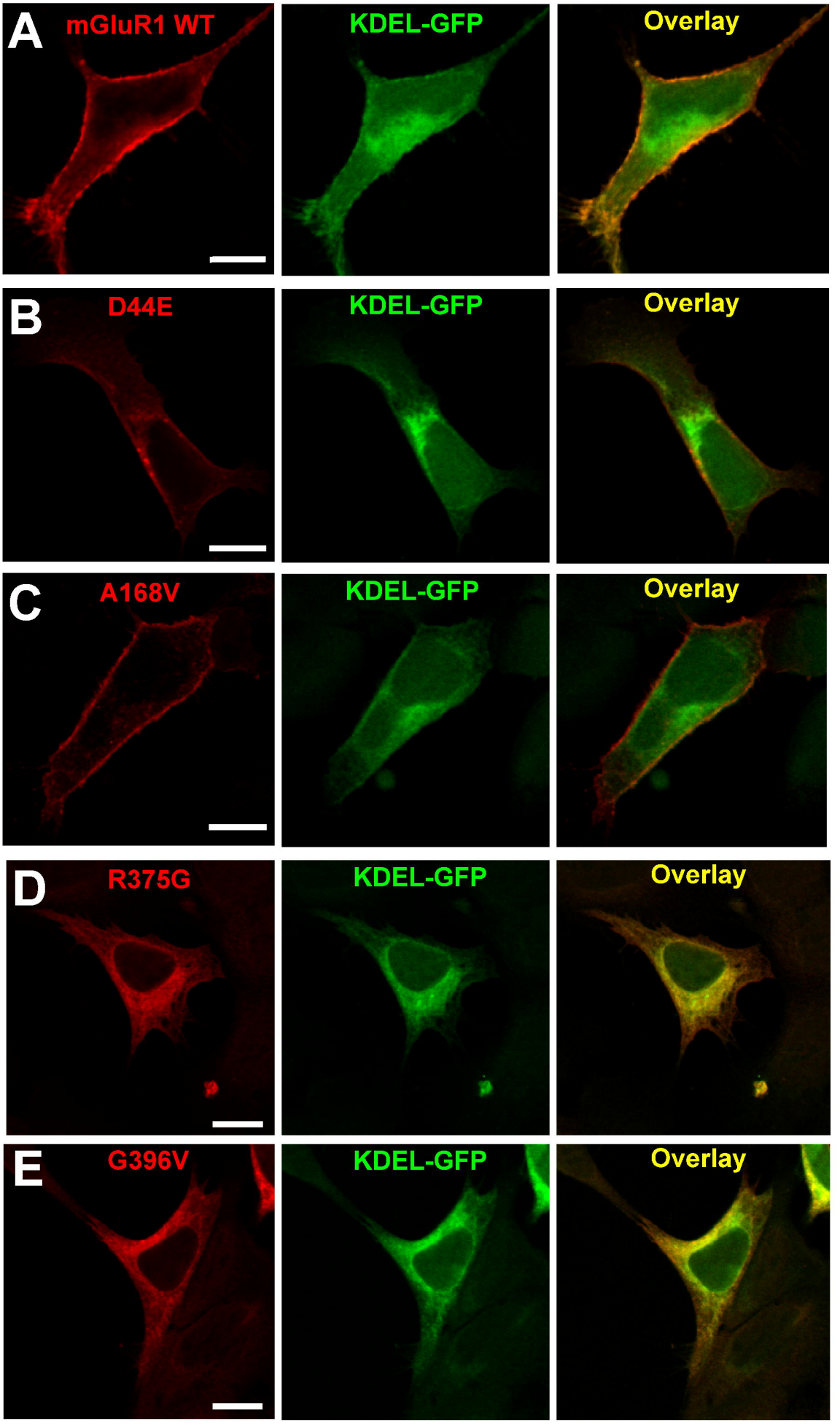
A
mGluR1 WT
KDEL-GFP
Overlay
B
D44E
KDEL-GFP
Overlay
C
A168V
KDEL-GFP
Overlay
D
R375G
KDEL-GFP
Overlay
E
G396V
KDEL-GFP
Overlay

Figure 4

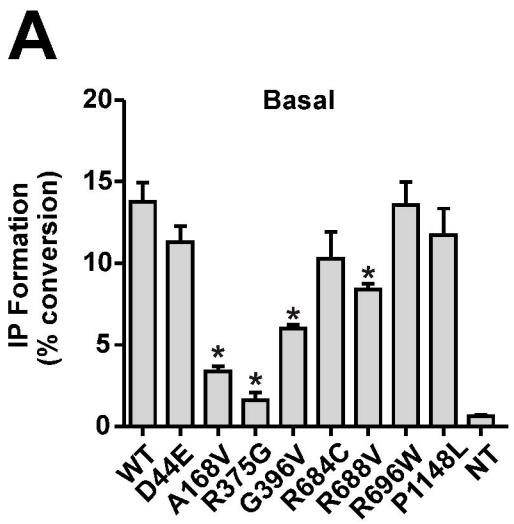
A
Basal
IP Formation (% conversion)
20
15
10
5
0
WT
D44E
A168V
R375G
G396V
R684C
R688V
R696W
P1148L
NT

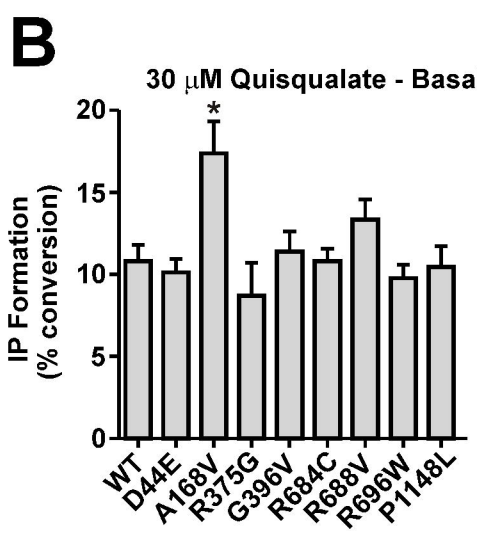
B
30 μM Quisqualate - Basal
IP Formation (% conversion)
20
15
10
5
0
WT
D44E
A168V
R375G
G396V
R684C
R688V
R696W
P1148L

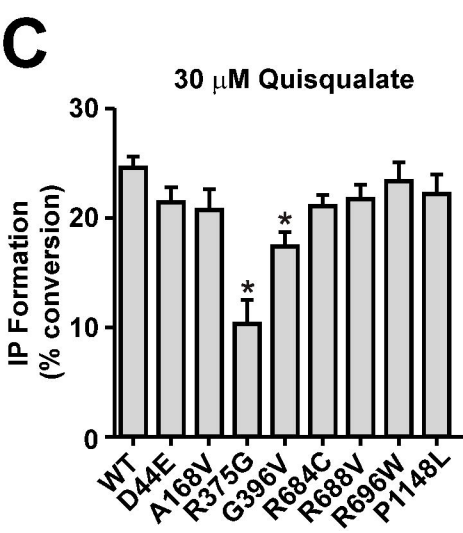
C
30 μM Quisqualate
IP Formation (% conversion)
30
20
10
0
WT
D44E
A168V
R375G
G396V
R684C
R688V
R696W
P1148L

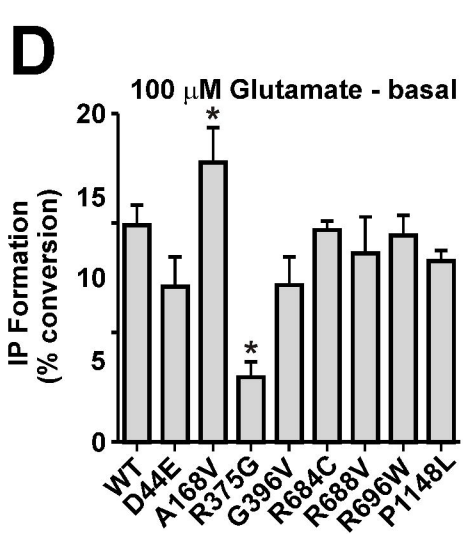
D
100 μM Glutamate - basal
IP Formation (% conversion)
20
15
10
5
0
WT
D44E
A168V
R375G
G396V
R684C
R688V
R696W
P1148L

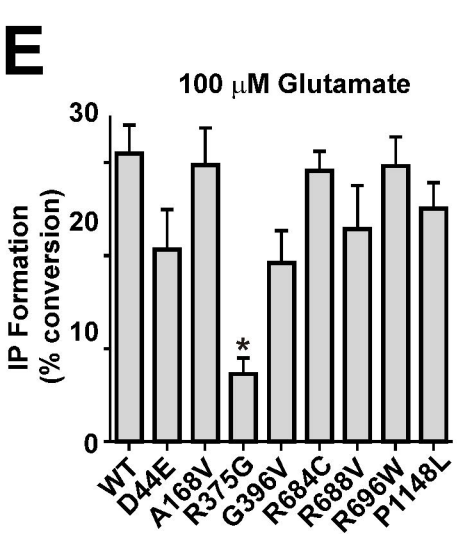
E
100 μM Glutamate
IP Formation (% conversion)
30
20
10
0
WT
D44E
A168V
R375G
G396V
R684C
R688V
R696W
P1148L

Figure 5

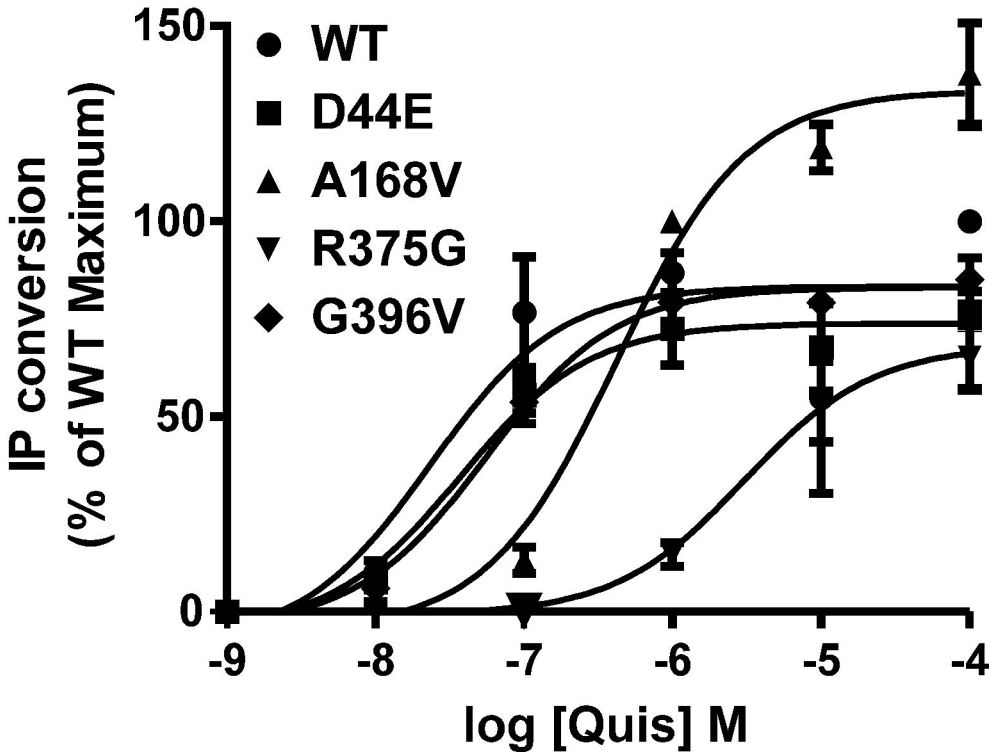
150
100
50
0
IP conversion
(% of WT Maximum)
WT
D44E
A168V
R375G
G396V
-9
-8
-7
-6
-5
-4
log [Quis] M

Figure 6

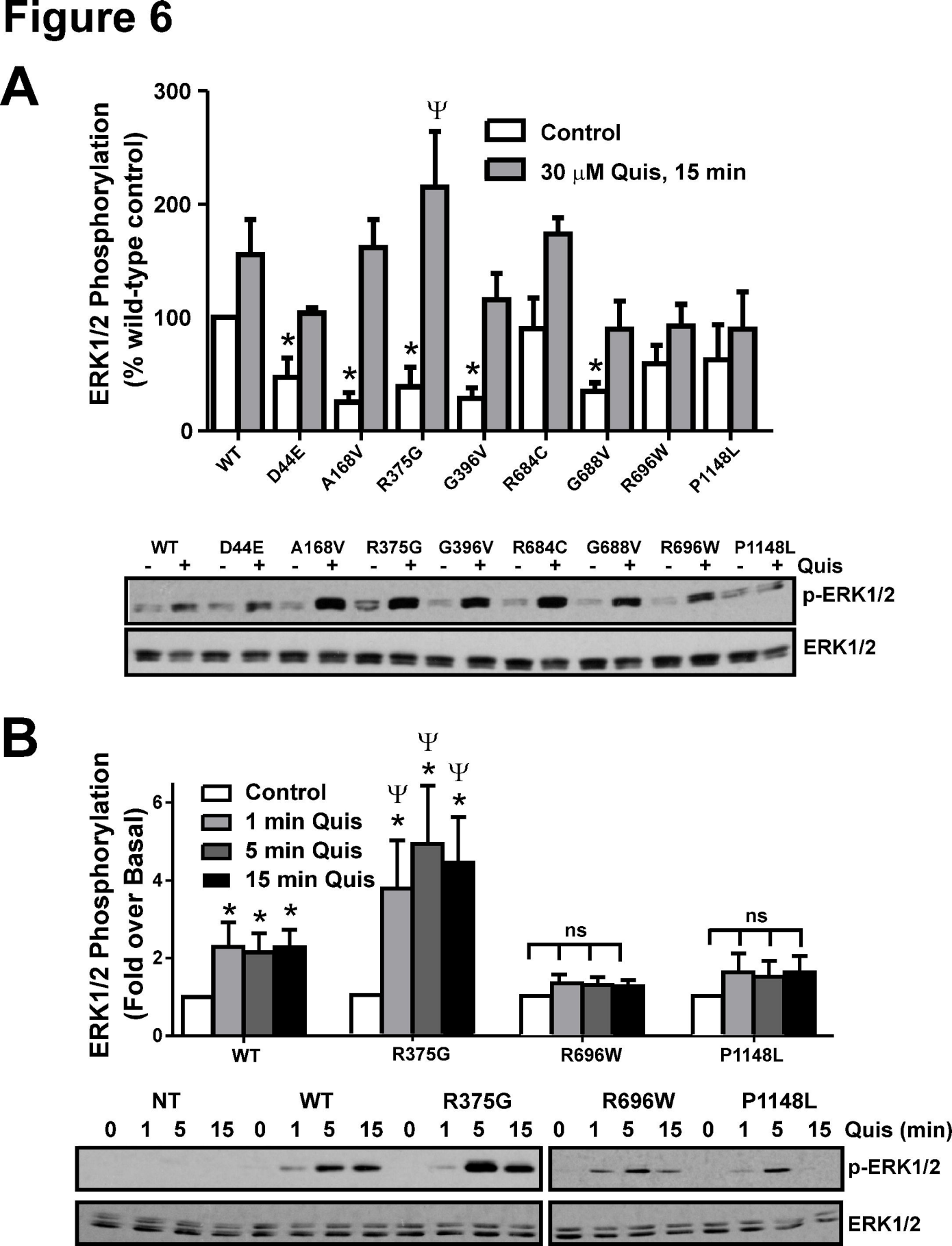
A
ERK1/2 Phosphorylation (% wild-type control)
300
200
100
0
Control
30 μM Quis, 15 min
Ψ
*
WT
D44E
A168V
R375G
G396V
R684C
G688V
R696W
P1148L
Quis
p-ERK1/2
ERK1/2
B
ERK1/2 Phosphorylation (Fold over Basal)
6
4
2
0
Control
1 min Quis
5 min Quis
15 min Quis
ns
NT
0 1 5 15 0 1 5 15 0 1 5 15 0 1 5 15 0 1 5 15 Quis (min)

Figure 7

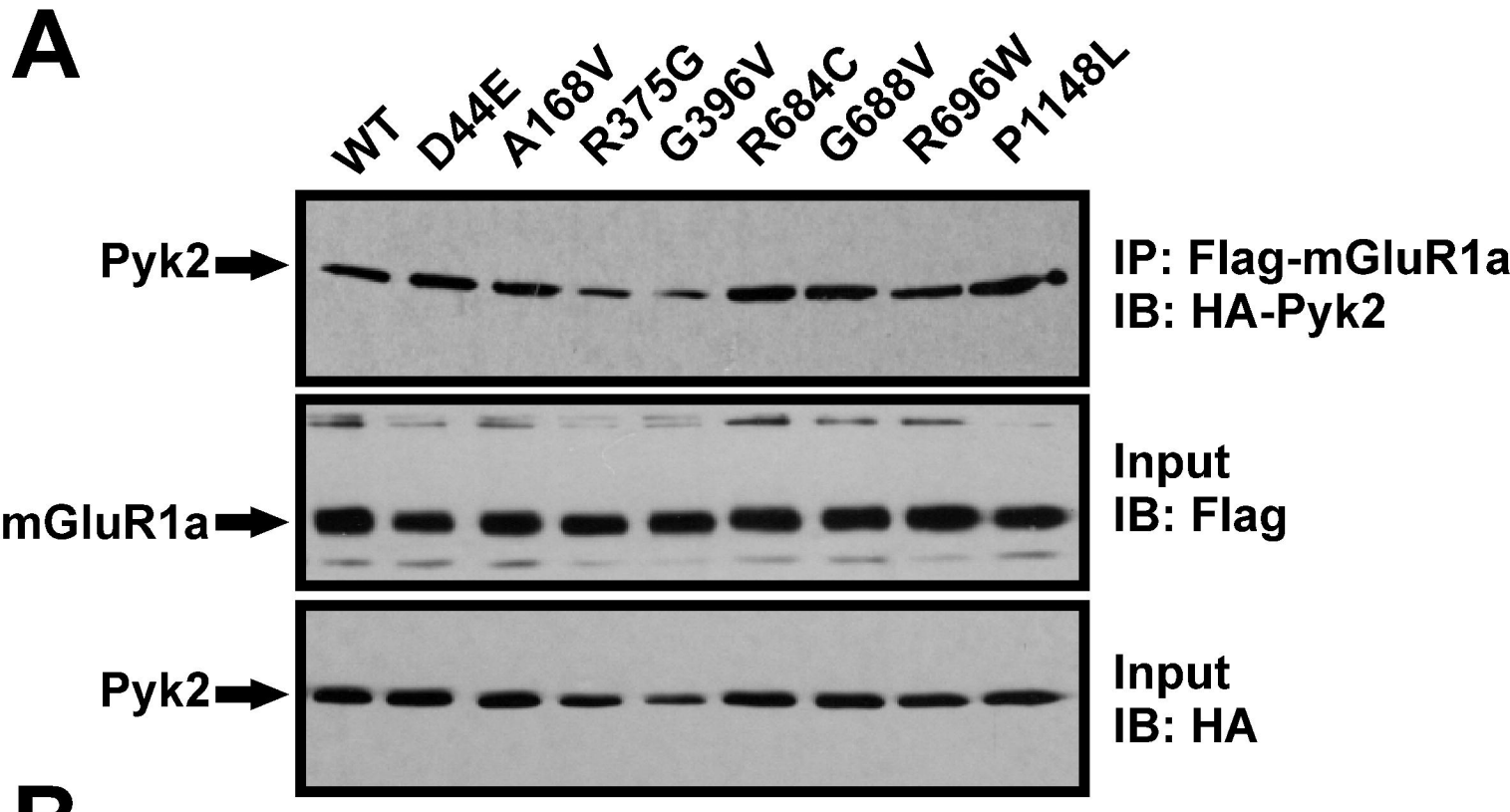
A
WT
D44E
A168V
R375G
G396V
R684C
G688V
R696W
P1148L
Pyk2
IP: Flag-mGluR1a
IB: HA-Pyk2
mGluR1a
Input
IB: Flag
Pyk2
Input
IB: HA

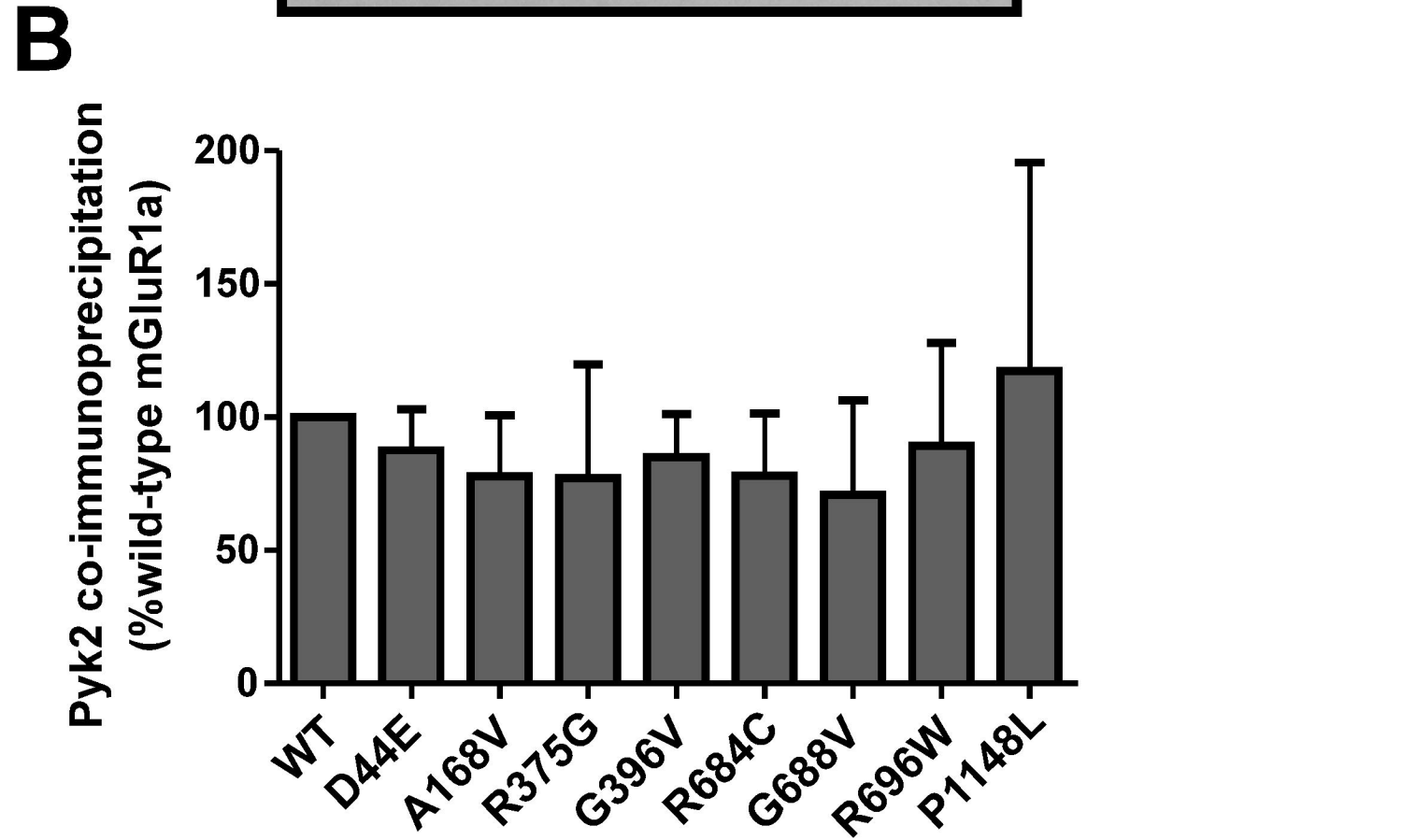
B
Pyk2 co-immunoprecipitation
(%wild-type mGluR1a)
200
150
100
50
0
WT
D44E
A168V
R375G
G396V
R684C
G688V
R696W
P1148L

Figure 8

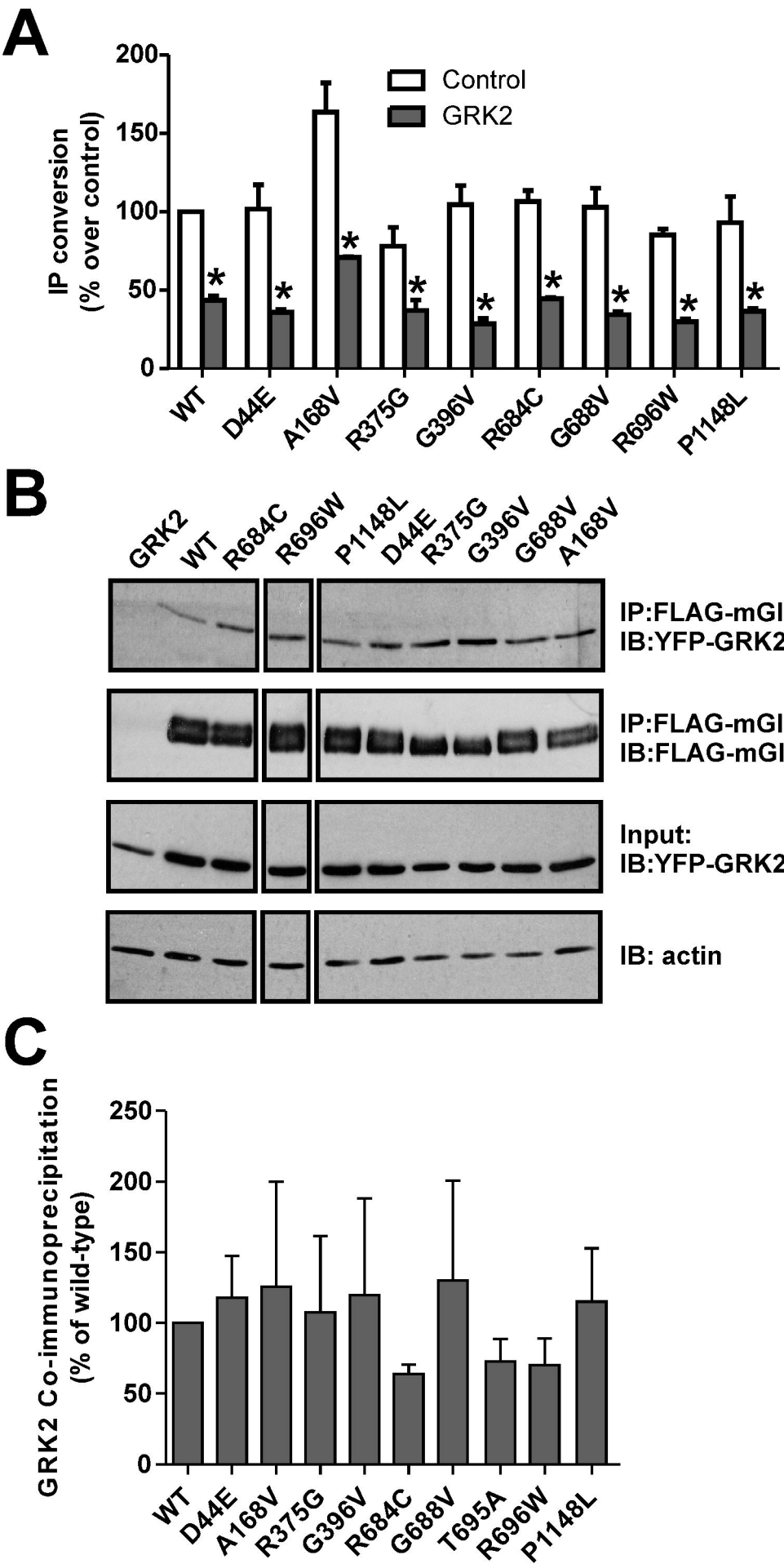
A
IP conversion (% over control)
200
150
100
50
0
Control
GRK2
*
WT
D44E
A168V
R375G
G396V
R684C
G688V
R696W
P1148L
B
GRK2
WT
R684C
R696W
P1148L
D44E
R375G
G396V
G688V
A168V
IP:FLAG-mGluR1
IB:YFP-GRK2
IP:FLAG-mGluR1
IB:FLAG-mGluR1
Input:
IB:YFP-GRK2
IB: actin
C
GRK2 Co-immunoprecipitation (% of wild-type)
250
200
150
100
50
0
WT
D44E
A168V
R375G
G396V
R684C
G688V
T695A
R696W
P1148L

Figure 9

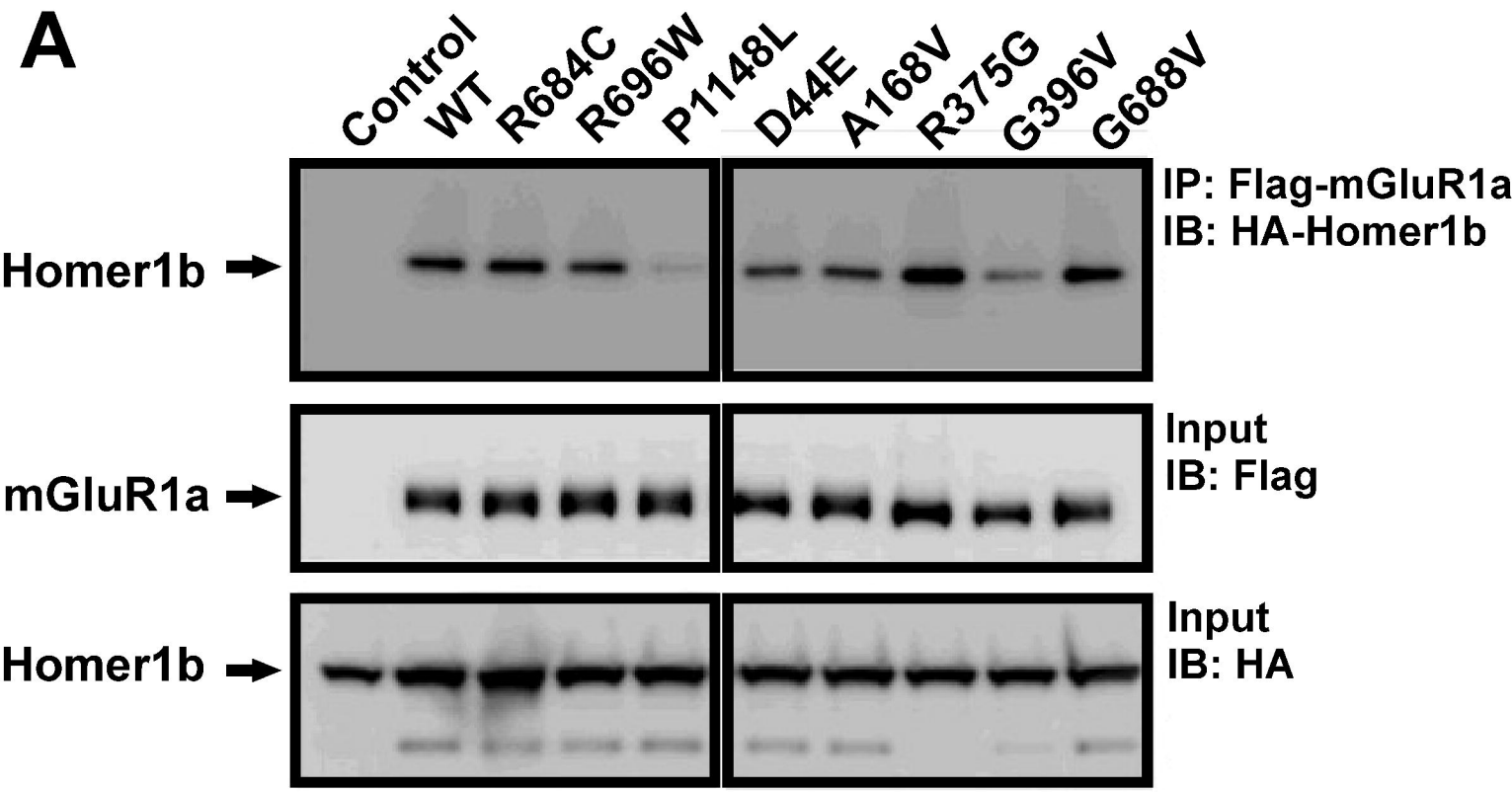
A
Control
WT
R684C
R696W
P1148L
D44E
A168V
R375G
G396V
G688V
Homer1b
IP: Flag-mGluR1a
IB: HA-Homer1b
mGluR1a
Input
IB: Flag
Homer1b
Input
IB: HA

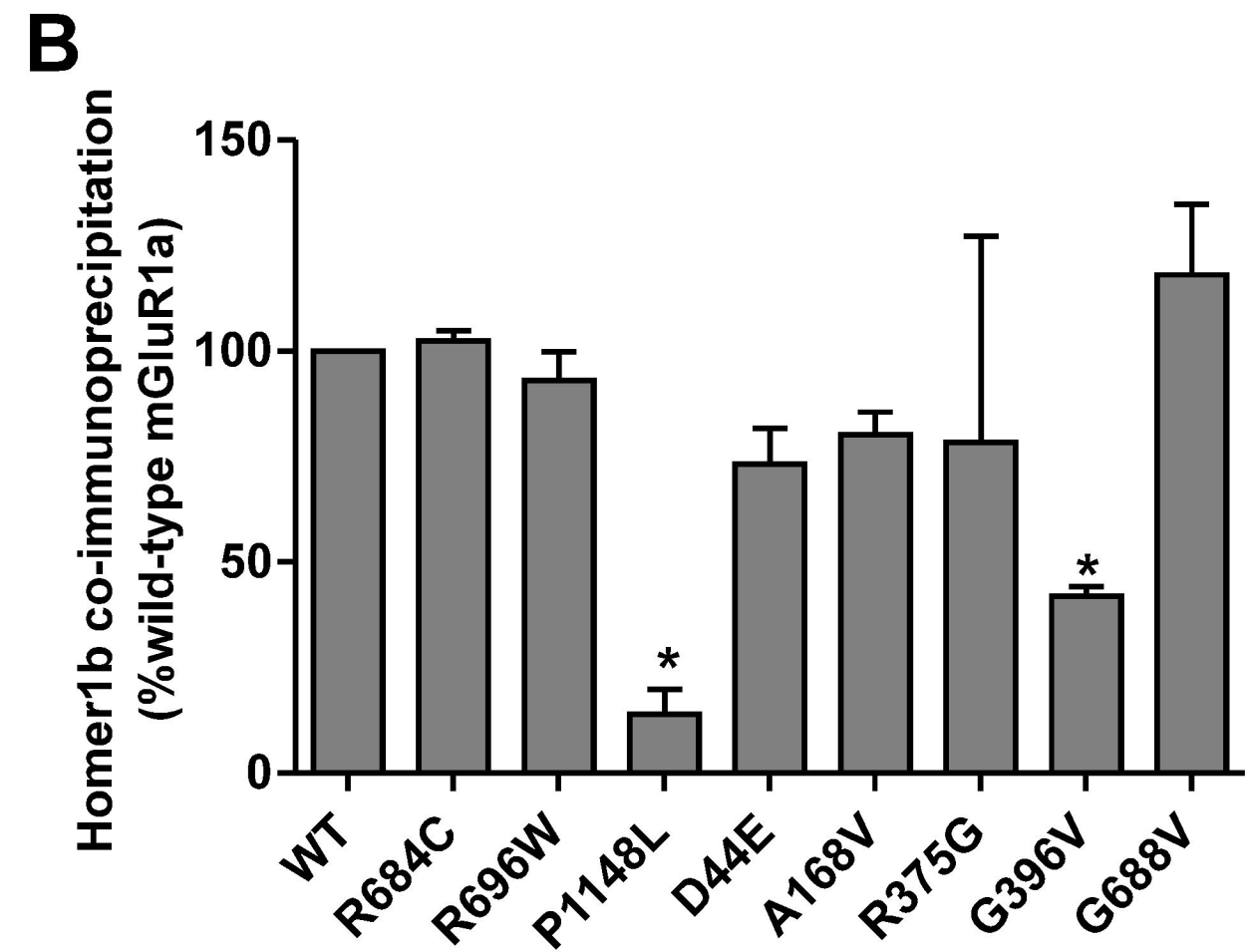
B
Homer1b co-immunoprecipitation
(%wild-type mGluR1a)
150
100
50
0
*
*
WT
R684C
R696W
P1148L
D44E
A168V
R375G
G396V
G688V

Figure 10

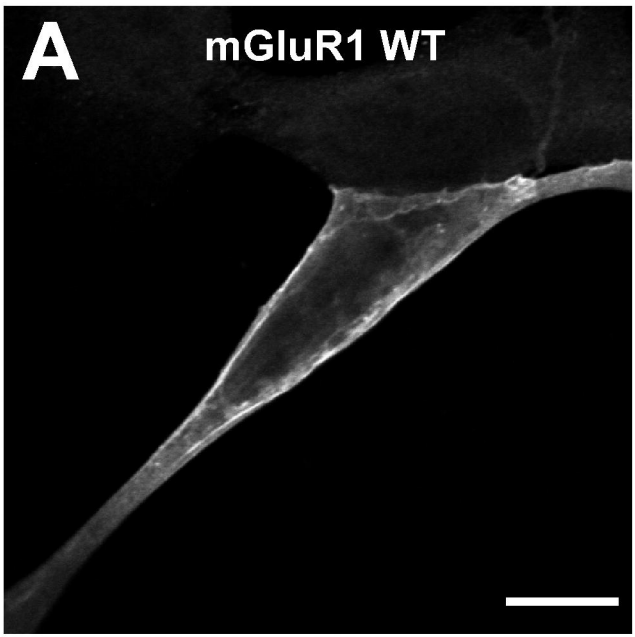
A
mGluR1 WT

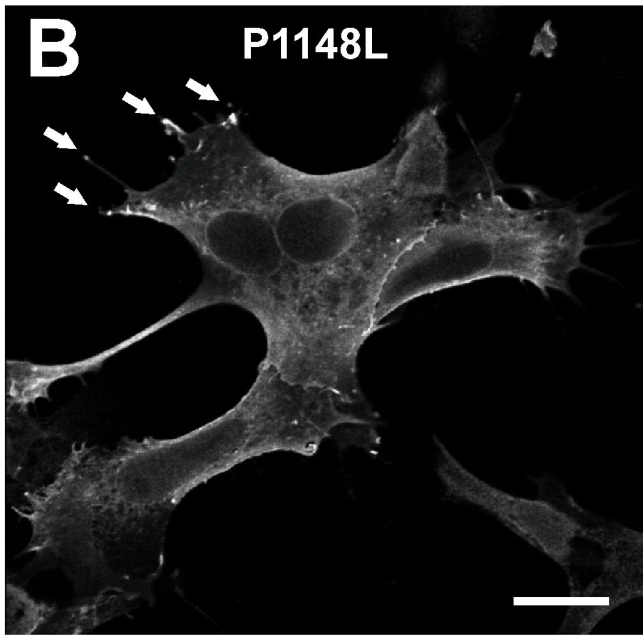
B
P1148L

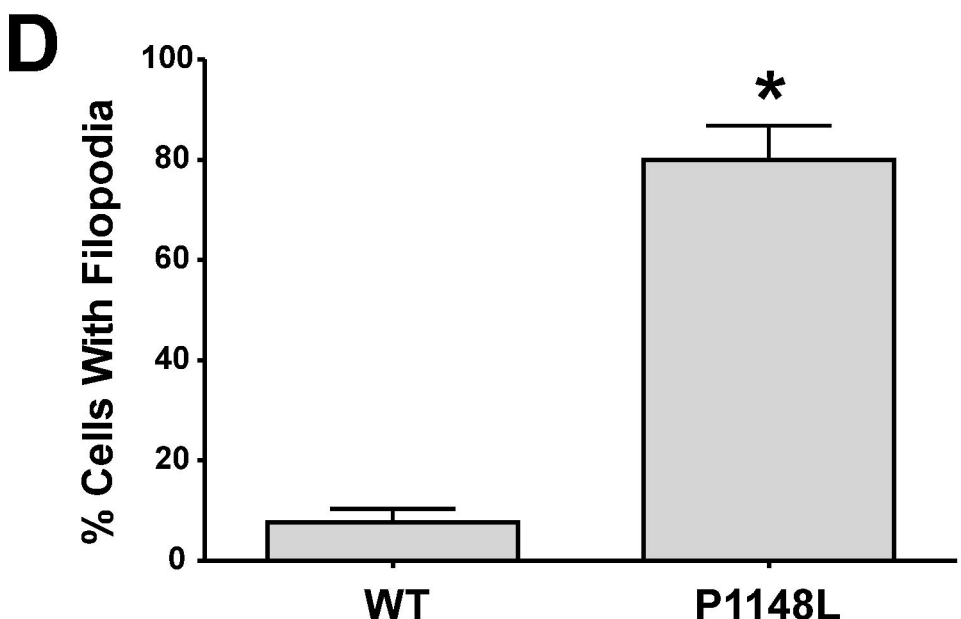
D
% Cells With Filopodia
100
80
60
40
20
0
*
WT
P1148L